Charles University in Prague
Faculty of Sciences

Study program: Biology

Darina Šikrová

Functional analysis of eIF3e subunit of human translation initiation factor 3 in living cells

Funkční analýza eIF3e podjednotky lidského translačního iniciačního faktoru eIF3 v živých buňkách

Diploma Thesis

Supervisor: Leoš Valášek, PhD

Prague, 2015

Declaration

Hereby, I declare that I have written the submitted thesis myself and I have used no other information sources than those appropriately cited, nor have I used other materials or aids than those indicated. This work or any of its substantial part was not and will not be used for obtaining any other academic degree.

In Prague..... .....

Darina Šikrová

Acknowledgments

I dedicate the first gratitudes to my parents for all the love and care I am blessed to receive from them. For this a child cannot render formal thanks in formal words.

My second sincere thank you goes to my supervisor Leoš Valášek, Ph.D., not only for his scientific, but also personal guidance and for giving me the opportunity to work in such a joyful and friendly environment among great people. And so, I would like to extend this appreciaiton also to other members of the LRGE group, namely Slávka Gunišová, Petra Beznosková, Jakub Zeman, Vlaďka Vlčková, Myrte Jansen, Mahabub Pasha, Olga Krýdová and especially to Anička Herrmannová and Susan Wagner, who both have been incredible help to me and that the time spent in the cold room did not feel so cold, actually.

And at last (but so not the least), I would like to thank to all of the amazing members of Cochella (worm´s) group at the Institute of Molecular Pathology, namely Luisa Cochella, Ph.D, Chiara Alberti, Susanne Bloch, Thomas Danielle, Tanja Drexel and Thomas Steinacker who have helped me to grow exponentially during my four Viennese months. So for that and so much more – muchas gracias, grazie mille, merci beaucoup and danke schön.

Abstract

Eukaryotic initiation factor 3 (eIF3) is a critical player involved in many steps of translation initiation, which ultimately result in the formation of the elongation competent 80S ribosome. With its 13 subunits (eIF3a – eIF3m) it is the largest and the most complex translation initiation factor composed of three mutually interconnected modules (i - iii), however, the role of individual subunits involved in its structural integrity and proper function is not fully explored. The eIF3e subunit was shown to be a part of the human eIF3 structural core and to help in the mRNA recruitment to the 43S pre-initiation complex by forming a molecular bridge between the 40S ribosomal subunit and the mRNA cap-binding complex. In this study, we employed siRNA-directed downregulation of eIF3e in HeLa cells and analysed its impact on the overall eIF3 integrity and function *in vivo*. The eIF3e knock-down ($eIF3e^{K.D.}$) led to the severe reduction of protein amounts of other three subunits (eIF3d, k and l), which together with the subunit eIF3c and e form module ii of the eIF3 complex. Remaining module i (composed of a, b, g and i) and iii (containing f, h and m) stayed partially bound perhaps thanks to a bridging effect of eIF3c, and showed reduced binding efficiency towards the 40S subunit compared to control cells. Furthermore, eIF3e-depleted cells exhibited decreased translation initiation rates and slow growth. The observed phenotype of the $eIF3e^{K.D.}$ indicates that e subunit of human eIF3 is important for the integrity of the complex, its ability to bind to small ribosomal subunit and thus to the overall fitness of cells.

Key words: eukaryotic translation initation, eIF3, eIF3e, siRNA-directed knock-down

Abstrakt

Eukaryotický iniciační faktor 3 (eIF3) je významným hráčem zúčastňujícim se více kroků iniciace translace, která v konečném důsledku vede k vytvoření elongace-schopného 80S ribosómu. Se svými 13 podjednotkami (eIF3a – eIF3m) představuje největší a nejkomplexnější translační iniciační factor, který se skládá ze tří vzájemně popřepájených modulů (i - iii). Navzdory jeho bezesporné důležitosti, přínos jednotlivých podjednotek pro jeho struktúrní integritu a správnou funkci není plně proskúmaný. Bylo zjistěné, že eIF3e podjednotka je součásti oktamerního jadra lidského eIF3 komplexu a navyše bylo proukázané, že je komponentem molekulárního přemostění mezi 40S ribosomální podjednotkou a čepička-vazebným komplexem, čím tak napomáha vazbě mRNA na 43S preiniciační komplex. V této práci byl analyzovaný dopad siRNA navozenej zníženej exprese eIF3e podjednotky na integritu a funkci eIF3 v *in vivo* podmínkach. Znížení tvorby eIF3e, tzv. eIF3e knock-down ($eIF3e^{K.D.}$), vedlo k výraznýmu úbytku dalších 3 podjednotek (d, k a l), které spolu s podjednotkami c a e tvoří modul ii lidského eIF3 komplexu. Zvyšné moduly i (obsahujíci a, b, g a i) a iii (pozostávajíci z f, h a m) ostali sčásti spolu asociované pravděpodobně za pomoci eIF3c a ich vazebná afinita voči 40S podjednotce klesla. Navyše buňky s nedostatkem eIF3e vykazovali zníženou účinost iniciace translace a pomalší rast. Pozorovaný fenotyp $eIF3e^{K.D.}$ buňek naznačuje, že e podjednotka lidského eIF3 je důležitá pro celistvost tohto komplexu, jeho schopnost vázat se na malou ribosomální podjednotku a taktéž celkovou životaschopnost buňek.

Klíčová slova: eukaryotická iniciace translace, lidský eIF3, eIF3e, siRNA-navozená snížená exprese

Table of Contents

List of Abbreviations

43S/48S PIC	43S or 48S pre-initiation complex
5´ UTR	5´ untranslated region
A-site	aminoacyl tRNA site
A_x	absorbance measured at a certain wavelength (x) in nm
B2-MG	β2-microglobulin
BSA	bovine serum albumin
CTD	C-terminal domain
CoIP	coimmunoprecipitation
Cryo-EM	cryo-electron microscopy
DMEM	Dulbecco´s modified Eagle´s medium
eIFx	eukaryotic initiation factor (x substitutes a concrete number)
eIF3a – m	a – m respective subunit of eIF3
$eIF3x^{K.D.}$	knock-down of eIF3x subunit (x substitutes a concrete subunit)
E-site	exit tRNA site
FBS	foetal bovine serum
INT6	integration site 6 protein
IRES	internal ribosome entry site
MFC	multifactor complex
MPN	Mpr1-Pad1-N-terminal domain
MS	mass spectrometry
MTT	3-[4,5-dimethylthiazol-2-yl]-2,5 diphenyl tetrazolium bromide
Mnk1	MAPK signal integrating kinase 1
NMD	nonsense-mediated mRNA decay pathway
NT	non-targeting siRNA
NTD	N-terminal domain
ORF	open reading frame
P/M ratio	polysome-to-monosome ratio
PABP	poly-A binding protein
PBS	phosphate-buffered saline
PCI	Proteasome-COP9-eIF3 domain
P-site	peptidyl tRNA site
PTMs	post-translational modifications
RNA_i	RNA interference
RRM	RNA-recognition motif
RT	room temperature
SDS	sodium dodecyl sulphate
siRNA	small interfering RNA
PAGE	polyacrylamide gel electrophoresis
TBS	tris-buffered saline
TBS-T	tris-buffered saline with added Tween 20
TC	ternary complex
$tRNA_i$	initiator tRNA
WCE	whole-cell extract
WHD	winged helix domain

Introduction

Protein synthesis and regulation of gene expression represent the core of molecular biology, whose main object is to study how genetic instructions encode for biological function. Since deciphering the first „word“of genetic code by Nirenberg and Matthaei, there have been tremendous advances in elucidating the sophisticated machinery responsible for the translation of genes. However, our understanding of respective molecular events still faces many challenges, especially with ever-growing evidence for the increasing complexity of gene regulatory networks.

One of the critical regulation steps of gene expression is translation initiation. It is also the most controlled phase of the whole translational cycle and by this it can account for more rapid changes in cell´s proteome as compared to the regulation on the transcriptional level.

The proper initiation of translation requires a coordinative interplay of many factors. The eukaryotic initiation factor 3 (eIF3) is perceived as one of the key players of this event, bridging individual components and thus interconnecting distinct sub-steps necessary for protein synthesis start. Most of our knowledge about eIF3 comes from genetic and biochemical studies in budding yeast. However, in the last decade there has been a great effort to focus also on its mammalian, more complex, counterpart and it is hoped that upcoming years will form a better view of the functional roles of mammalian eIF3 subunits and how they interact with each other to form the 13-subunit complex. This study focuses on one eIF3 subunit, namely eIF3e, and investigates the consequences on eIF3 assembly and functionality in translation initiation upon the depletion of this subunit in HeLa cells.

Literature Review

1 Mechanism of eukaryotic translation initiation

Translational control of gene expression represents critical regulatory means in cellular physiology or fate (Sonenberg & Hinnebusch, 2009). In all three kingdoms of life, translation consists of four ordered events: initiation, elongation, termination and renewal of free ribosome pool termed ribosome recycling. During initiation phase an initiator tRNA is located in the P-site of small ribosomal subunit, which itself is positioned at the correct initiation codon (prevalently AUG) of mRNA. Such state can then lead to the translation of a downstream open reading frame (ORF).

Translation initiation has been considered for a long time, as also already stated in the Introduction, as the rate-limiting step of translation for the majority of mRNAs. Indeed, recent studies from yeast, which have taken advantage of a newly developed method to monitor translational state *in vivo* - ribosome profiling, are in agreement with this longstanding view (Pop et al., 2014; Shah et al., 2013). Hence, the levels of endogenous protein will mostly depend on the competition between mRNAs for limiting pool of free ribosomes and successful assembly of translational apparatus. There are also other factors in game that can modulate translation by influencing polypeptide elongation rates instead of for example enhancing the translational speed of highly expressed genes via biased codon usage (Akashi, 2003). However, the optimization mechanisms that act during elongation phase can influence the pace of protein production only if the successful initiation event is accomplished.

1.1 Overview of cap-dependent translation initiation

Majority of cellular mRNAs in eukaryotes undergo the process of start codon selection by cap-dependent ribosomal scanning (Hinnebusch, 2011). During initiation, 40S ribosomal subunit preloaded with Met-$tRNA_i$ is recruited to the 5´ end of capped mRNA and the bases in the 5´ untranslated region (5´ UTR) are subsequently examined in the P-site of the ribosome to detect complementarity with the triplet anticodon of initiator tRNA ($tRNA_i$). After a successful recognition of the start codon, initiation culminates with binding of 60S subunit to 40S subunit leading to the formation of 80S initiation complex. This so-called scanning model of translation initiation has been acknowledged for almost 40 years now (Kozak, 1978). A schematic representation of the initiation pathway is overviewed in Fig. 1.1.

Small ribosomal subunit is a dynamic protein complex that undergoes many conformational changes during the process of translation initiation (Fraser & Doudna, 2007). Adopting and stabilizing a specific conformation for a concrete sub-step of initiation pathway requires the help of initiation factors, with the first of them being identified in 1970s.

The 40S subunit can be subdivided into two large domains, the head and the body, with mRNA decoding site extending across their interface (Fig. 1.2 A). Prior the mRNA recognition and its recruitment to the ribosome, the 43S pre-initiation complex (43S PIC) needs to be assembled comprising the 40S subunit itself and additional 5 initiation factors (eIF1, eIF1A, eIF2•GTP•Met-tRNA$_i$, eIF3 and eIF5). During this assembly, 40S subunit adopts so-called open conformation with accessible mRNA decoding site. In the current model, initiation factors eIF1 and eIF1A are thought to cooperatively bind in a close proximity to the P- and A- sites, respectively, and induce the isomerization of 40S subunit to its open state by rotating its head clockwise by 8° (Fig. 1.2B) (Hussain et al., 2014).

The largest initiation factor, eIF3, resides mainly on the solvent site of 40S subunit but some of its subunits protrude further and thus encircle the upper body and head region of the 40S subunit. This allows eIF3 to make contacts with other factors at both ends of the mRNA channel and so engage in crosstalk between individual events happening during initiation on the opposite sites of translational machinery (Erzberger et al., 2014; Hashem et al., 2013).

The position of eIF5 is somewhat unclear due to its omission in many structural reconstitutions. Consistent with its known role as a GTPase activating protein (GAP) for eIF2 and its communication with eIF1 and 1A (Luna et al., 2012; Maag et al., 2006), recent cryo-EM reconstruction in yeast indicated its potential location on the surface of the 40S subunit, connecting eIF1 and γ subunit of eIF2 (Hussain et al., 2014). Although recent structures greatly improved our knowledge about location and interaction between individual eIFs, all of them came from only partially reconstituted pre-initiation complexes always lacking some of the factors.

The delivery of Met-tRNAi occurs via ternary complex (TC) composed of GTP bound eIF2 and Met-tRNAi. Its binding to the ribosomal P-site is promoted and further stabilized by eIF1, eIF3 and eIF5 (Majumdar et al., 2003; Sokabe et al., 2012). However, the sequence in which individual initiation factors bind to the 40S subunit is to date unsure. It seems that there is not just one possible route how the 43S PIC can be assembled.

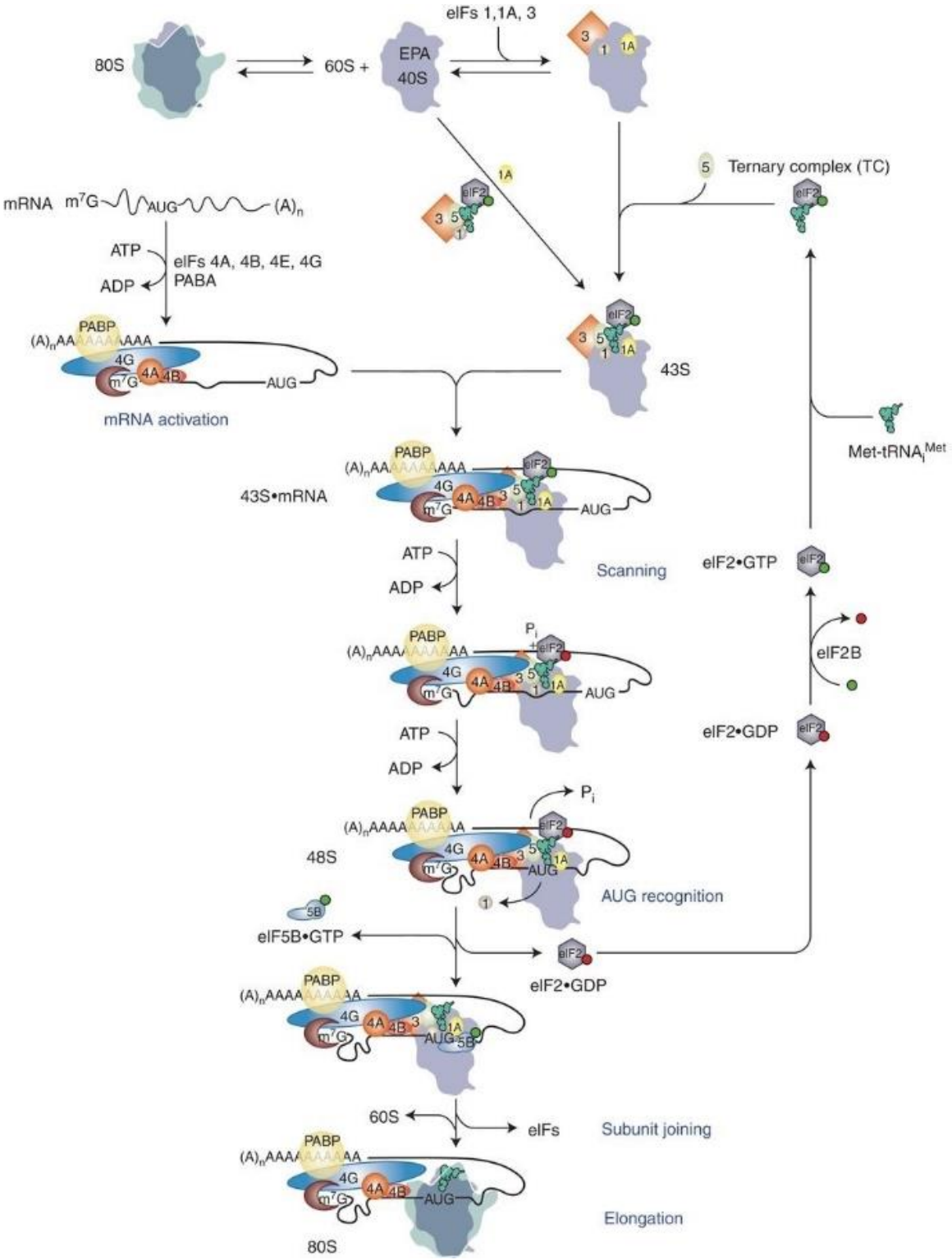

Figure 1.1 Schematic representation of canonical eukaryotic initiation pathway. Initiation begins with recycling of post-termination ribosomes. Ternary complex containing eIF2•GTP•Met-tRNAi is then loaded on the free 40S subunit with the help of additional initiation factors (1, 1A, 3 and 5), forming 43S pre-initiation complex. Meanwhile, eIF4 factors and PABP bind to the 5´cap of mRNA, causing the mRNA to loop and adopt the activated form. 43S PIC recognizes cap complex and once bound on the 5´ end of mRNA it starts the scanning process to locate initiation codon. Recognition of proper start codon triggers hydrolysis of eIF2-bound GTP and leads to the arrest of 40S subunit, followed by eIF5B•GTP mediated joining of 60S subunit. 80S formation is completed with hydrolysis of GTP by eIF5B and dissociation of initiation factors (figure adapted from Hinnebusch & Lorsch, 2012).

One scenario deals with a stable intermediate, the so-called multifactor complex (MFC), which consists of eIF1, eIF2, eIF3 and eIF5 and is assembled before its binding to the small ribosomal subunit. Its ability to exist free of the 40S ribosome was first reported from yeast (Asano et al., 2000) and later on, similar MFCs were detected also in plants and mammals (Dennis et al., 2009; Sokabe et al., 2012). Another way of the 43S PIC formation is individual binding of MFC components to 40S subunit. This seems especially likely as eIF3 was reported to help dissociation of terminating ribosomes and to prevent premature joining of 40S and 60S subunits (Kolupaeva et al., 2005), suggesting that perhaps it may bind first and help to recruit other factors. If these different pathways work in parallel within a cell or if one is dominant over the other still needs to be answered. Nevertheless, the binding of initiation components is thermodynamically coupled and there is an important cooperativity among individual factors affecting each other´s affinity for 40S ribosome (Sokabe & Fraser, 2014).

Next step after the 43S PIC assembly is the recruitment of mRNA, which results in formation of the 48S pre-initiation complex (48S PIC). During this event, another initiation factor complex comes into play, eIF4F, whose activity was first identified in the reconstituted reticulocyte translation system (Grifo et al., 1983). It represents a connecting point between the mRNA and the 43S PIC by binding to the 7-methyl-guanosine cap of mRNA. This complex is composed of three subunits: the cap-binding protein - eIF4E, the scaffold protein - eIF4G and the DEAD-box helicase - eIF4A.

eIF4E is the main factor responsible for the cap recognition by using three conserved tryptophan residues to intercalate the 5´ modified guanosine of mRNA (Joseph Marcotrigiano et al., 1997). Its availability in the cell is controlled by the family of eIF4E binding proteins (4E-BPs), which act as binding competitors of eIF4G, thus preventing a full eIF4F complex formation (Richter & Sonenberg, 2005). Such binding intervention is dependent on the phosphorylation event. Non-phosphorylated 4E-BP interacts tightly with eIF4E, while its multiple phosphorylation leads to the sequestration of eIF4E binding site (Bah et al., 2014).

eIF4G acts as a bridge between eIF4E and eIF4A and on top of that it possesses also binding domains for RNA, eIF3 and poly-A binding protein (PABP) (Korneeva et al., 2000; J Marcotrigiano et al., 2001; Tarun & Sachs, 1996). It is thought that interaction between eIF4E-bound mRNA, eIF4G and PABP enables assembly of mRNA closed-loop structure (Wells et al., 1998), which is assumed to be important for the 43S PIC attachment during multiple rounds of translation on the same mRNA molecule.

eIF4A is the ATP-dependent RNA helicase and its role is to "iron out" any possible cap-proximal secondary structures of mRNA for the efficient loading of the 43S PIC (Svitkin et al., 2001). It has not been clear whether its unwinding activity happens through a processive or distributive manner, but a new study revealed that eIF4A displays, in fact, a factor-mediated processivity (Garcia-Garcia et al., 2015). Previously, the RNA-unwinding activity was shown to be enhanced by two additional RNA-binding proteins – eIF4B and eIF4H (Rogers et al., 2001), but new data further show that any one of them together with 4G increases not only the mRNA unwinding efficiency but also the 5′-3′ directionality of eIF4A (Garcia-Garcia et al., 2015).

Loading of the 43S PIC to the mRNA in mammals is mediated mainly by the interaction between eIF4G and eIF3 (Villa et al., 2013; Walsh & Mohr, 2014). The resulting 48S PIC proceeds to the scanning process to look for the start codon in the appropriate sequence context (GCCRCCATGG, where R stands for purine) known as Kozak consensus sequence (Kozak, 1987). At least in higher eukaryotes, scanning through the more stable structures in mRNA requires, in addition to the eIF4F complex, a DExH-box helicase - DHX29 (Pisareva et al., 2008).

During scanning, $tRNA_i$ of TC is not fully accommodated in the P-site but is in the metastable (P_{OUT}) state that allows control of base-pairing between its anticodon and triplets entering the P-site (Fig. 1.2 C) (Saini et al., 2010). Upon recognition of the AUG start codon, $tRNA_i$ inserts deeper in the P-site, leading to the state dubbed P_{IN} (Saini et al., 2010), which evokes the rearrangement of factors bound to 40S subunit. eIF5 stimulates the hydrolysis of GTP bound eIF2 (Paulin et al., 2001) and the release of the inorganic phosphate (P_i) is enabled by the displacement of eIF1 and the C-terminal tail of eIF1A from their position near the P-site (Nanda et al., 2013). Codon-anticodon duplex is further stabilized by the N-terminal tail of eIF1A and the 48S PIC isomerizes to the closed, scanning arrested conformation by undergoing its head rotation by another 5° (Fig. 1.2D) (Hussain et al., 2014).

To complete translation initiation process, 60S subunit needs to join the arrested 48S PIC. This step is promoted by eIF5B, a GTPase that catalyses the second and last GTP hydrolysis during initiation. This second GTP hydrolysis was shown to be essential for the displacement of eIF5B from the resulting assembled 80S ribosome poised for elongation (Pestova et al., 2000).

For the next round of initiation, dissociated eIF2•GDP needs to be re-activated back to its •GTP form. This reaction is facilitated by eIF2B, which acts as a guanine nucleotide exchange factor for eIF2 (Gordiyenko et al., 2014; Panniers & Henshaw, 1983).

Even though ribosomes are the main catalysts of translational process, the kinetics of this reaction is greatly enhanced by the support of aforementioned additional factors. Moreover, they help to ensure that entire process of codon selection is accurate and they can also represent the targets for translational control of gene expression via their activation or inhibition as shortly described for eIF4E.

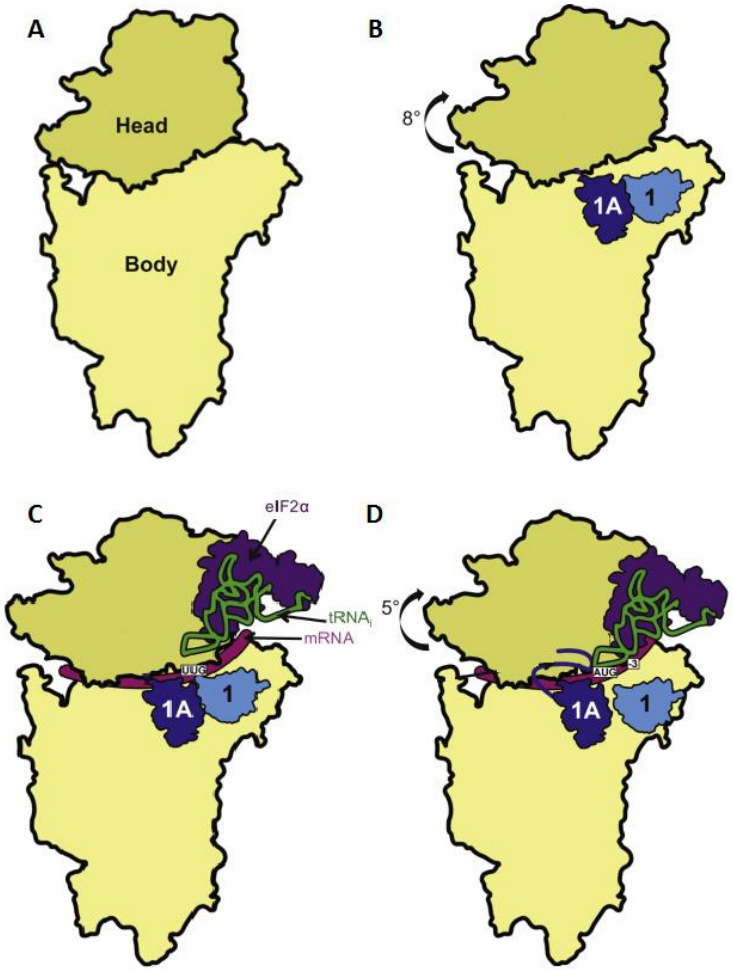

Figure 1.2 Schematic representation of the 40S ribosomal subunit´s conformational changes during distinct initiation steps viewed from the subunit interface site. Compared to the conformation of free 40S subunit (A), in the 43S PIC the head of 40S subunit is rotated by 8° (B), which allows binding of TC into the P-site in the P_{OUT} state (C). Recognition of the start codon leads to the deeper insertion of TC and further rotation of the head by 5° (D) (figure adapted and modified from Hussain et al., 2014).

2 Human eukaryotic initiation factor 3

eIF3 was one of the first discovered initiation factors back in 1970s (Benne & Hershey, 1976) and on top of that it has also surpassed other factors in the molecular mass and the composition complexity.

Mammalian eIF3, whose mass (~ 800 kDa) strikingly accounts for approximately two thirds of that of small ribosomal subunit (~ 1,200 kDa), is composed of 12 + 1 subunits, consecutively named eIF3a – m (Fig. 2.1B) (Browning et al., 2001; Damoc et al., 2007). The "+ 1" refers to eIF3j, which has been suggested not to be considered as *bona fide* eIF3 subunit anymore due to its functional diversity compared to the rest of the eIF3 complex. Several studies reported that eIF3j can readily dissociate from the rest of eIF3 during its purification (Fraser et al., 2004; Unbehaun et al., 2004). Also, in quiescent T lymphocytes, eIF3j was shown not to be associated with eIF3, but upon mitogenic stimulation it joined the complex and increased its binding efficiency to the 40S ribosome (Miyamoto et al., 2005). Such stabilizing effect of this subunit on the eIF3 association with the 40S subunit has also been observed by another studies (Fraser et al., 2004; Nielsen et al., 2006). Finally, eIF3j has been shown to have role also in the translation termination. When investigating the involvement of eIF3 in stop codon read-through in yeast, it was shown that eIF3j affects this process in the opposite manner than eIF3 (Beznosková et al., 2013).

For comparison, yeast counterpart of mammalian eIF3 comprises only 5 + 1 subunits, namely TIF32/a, PRT1/b, NIP1/c, TIF34/i, TIF35/g and HCR1/j (Fig. 2.1A) (Asano et al., 1998; Phan et al., 1998). As already indicated in their names, they all have their respective orthologues in mammals. This situation is, however, not general for all fungal lineages. Aforementioned eIF3 subunit composition is true for *Saccharomyces cerevisiae* (a budding yeast), but for example, *Schizosaccharomyces pombe* (a fission yeast) has in comparison to *S. cerevisiae* additional five subunits eIF3d, e, f, h and m, although they are probably not all incorporated to one complex, but could form two distinct 8-subunit complexes (Sha et al., 2009). eIF3 from the lower eukaryote *Neurospora crassa* resembles the most the mammalian one. All 13 orthologues of human eIF3 subunits were found to be present in this organism, even yielding identical EM structure of the complex (Smith et al., 2013). Interestingly, probably the simplest eIF3 can be found in a pathogenic excavate, *Giardia duodenalis*, in which, by bioinformatic analysis of its genome, only four sequences of conserved subunits were found – eIF3b, c, i and j (Nunes et al., 2014). However, findings of such bioinformatic analysis should still be biochemically validated as some subunits could be overlooked due to their extreme sequence divergence.

The five-subunit complex (without considering eIF3j) as present in *S. cerevisiae* has been proposed to represent the conserved eIF3 core complex necessary for global protein synthesis (Hinnebusch, 2006). Yet, the two major biochemical functions of yeast eIF3 in translation initiation, recruitment of the ternary complex and mRNA, could be carried out, at

least *in vitro*, mainly by a trimer composed of the largest subunits eIF3a, b and c (Phan et al., 2001).

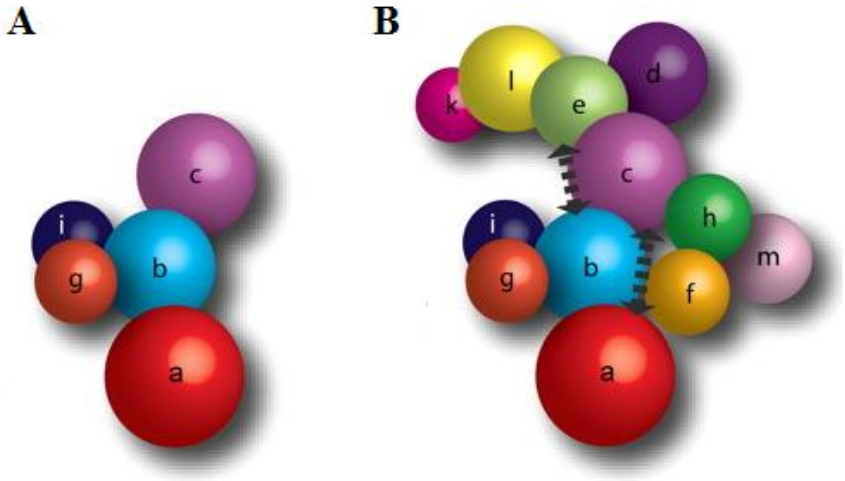

Figure 2.1 Subunit composition of budding yeast (A) and mammalian (B) eIF3, eIF3j not depicted. Dashed arrows indicate other interactions (pictures adapted from Zhou et al., 2008).

2.1 Architecture of human eIF3

First attempt to determine the spatial organization of native human eIF3 was a cryo-electron microscopy (cryo-EM) reconstruction in 2005 (Siridechadilok et al., 2005). The 30 Å-model shows eIF3 as a five-lobed structure displaying anthropomorphic features (Fig. 2.2A). The extending appendages are thus referred to as the body parts - head, arms and legs. Assembly of recombinant eIF3 (with truncated versions of subunits a (a*) and c (c*) lacking their terminal flexible domains) from subunits expressed in bacterial cells yielded a similar structure (Sun et al., 2011). Moreover, the study outlined the substeps of eIF3 complex formation. It seems, that subunits eIF3a and eIF3c act as a foundation stone by first forming a dimer and then, they further unite with another six subunits (e, f, h, k, l and m). The resulting stable octamer was proposed to be the structural core of human eIF3, to which the missing four subunits are serially added. Surprisingly, the cryo-EM structure of octamer bears a striking resemblance to the one of native eIF3 suggesting that other 4 subunits are linked in a rather flexible manner. Likely scenario is that b and d join individually and g and i as a dimer. eIF3j acted in a promiscuous manner by not showing clear binding preference. It was able to associate with a sole a*c* dimer, octameric complex as well as with subunits f and h. In contrast to this assembly pathway, salt-dependent disassembly of eIF3 followed by mass spectrometry (MS) revealed its disintegration into three stable modules designated as module i (a:b:g:i), module ii (c:d:e:k:l) and module iii (f:h:m) (Zhou et al., 2008). These modules were shown to be linked in this study by interactions

between subunits b:c and c:h. The role of eIF3c as a scaffolding subunit is consistent in both studies, however as eIF3b was shown to be dispensable for the formation of the stable eIF3 octamer, the more likely connecting interaction between module i and iii would seem to be between eIF3c and a, with eIF3b providing further stabilization support and in addition recruiting subunits eIF3g and i to the octamer. Indeed, spectrin (SPT) domain of eIF3a was shown to be a docking site for the formation of the subcomplex a:b:g:i (Dong et al., 2013). eIF3b and i bind concurrently to this domain, with eIF3g joining the subcomplex via its interaction with the C-terminal domain of eIF3b. The binding of eIF3b to eIF3a is mediated through its RNA-recognition motif (RRM). The same motif is, however, also recognized by eIF3j, leading to the mutually exclusive interaction of eIF3j and eIF3a with eIF3b.

The aforementioned MS experiment also revealed that the increasing ionic strength primarily leads to the disruption of the interaction between eIF3b:c and eIF3c:h suggesting that charged groups, like phosphorylated side-chains, could play role in some interactions among eIF3 subunits (Zhou et al., 2008). Indeed, 29 phosphorylation sites and several other post-translational modifications (PTMs) were identified within eIF3, with 7 of them found on eIF3b (Damoc et al., 2007). It will still need to be tested if some of these PTMs contribute to the intersubunit protein-protein interactions or play a role in translational regulation. It is however noteworthy, that module i together with eIF3c represents the core eIF3 complex from *S. cerevisiae*.

Querol-Audi et al. were able to assign subunits to regions within the eIF3 octameric core (Fig. 2.2B) (Querol-Audi et al., 2013). Intriguingly, similar overall shape and subunit organization is seen also in two other functionally unrelated macromolecular complexes – 19S proteasome lid and COP9 signalosome (Pick et al., 2009). Six subunits, in case of eIF3 - a, c, e, l, k and m, contain Proteasome-COP9-eIF3 (PCI) domain, which consists of a bundle of N-terminal α-helical repeats followed towards a C-terminus by a winged helix domain (WHD). Remaining two subunits, eIF3f and h, bear a Mpr1-Pad1-N-terminal (MPN) domain, which is predicted to adopt globular α/β folds (Enchev et al., 2010). PCI-domain containing subunits are thought to have the main architectural role as they laterally interact with their WHD domains to form a horseshoe-shaped structure at the base of the eIF3 octamer. As for the MPN subunits, seeing from their bridging position between left and right leg, they are proposed to be required for the stabilization of the core complex (Querol-Audi et al., 2013).

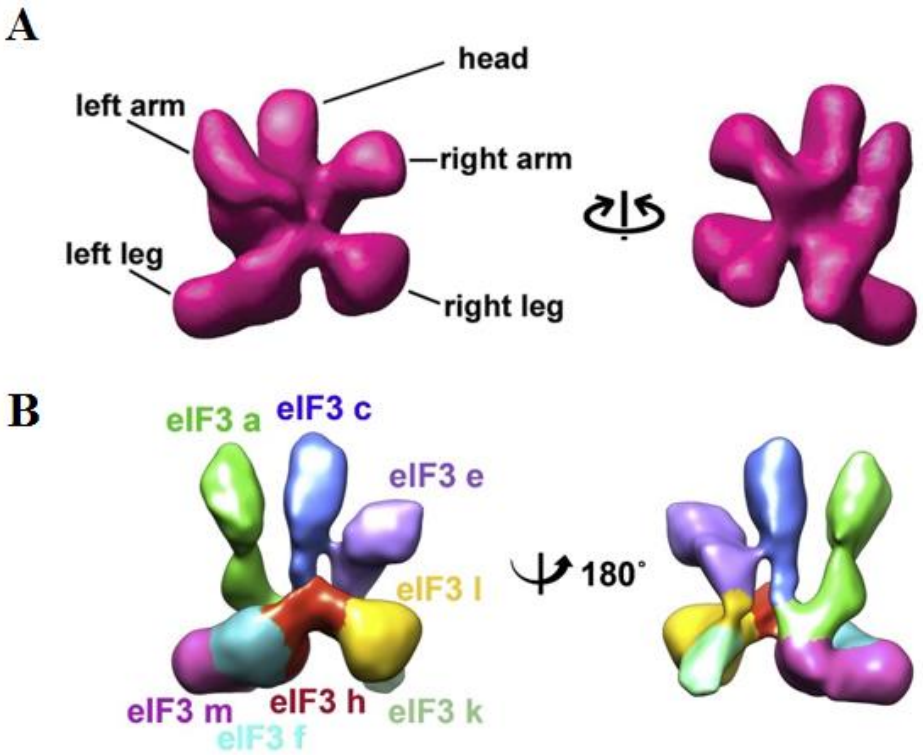

Figure 2.2 Cryo-EM reconstruction of natively purified intact eIF3 (A) and eIF3 octameric core (B). Front views of eIF3 are on the left and back views on the right side (pictures adapted from Siridechadilok et al., 2005 and Querol-Audi et al., 2013, respectively).

Other pieces to the eIF3 subunit-subunit interaction map were provided by the ablations of particular subunits. Specific knock-down of eIF3c severely reduced the protein levels of all module ii subunits, whereas eIF3a knock-down resulted in the dramatic loss of the whole octamer and eIF3d, in other words all module ii and iii subunits (Wagner et al., 2014). In addition to this, Zeng et al. have shown that eIF3m deficiency affects the protein levels of its two, module iii, binding partners (eIF3f and h) and eIF3c (Zeng et al., 2013). These data suggest that octameric view of eIF3 and proposed modularity do not contradict each other as the modules can still be recognized within the octamer.

2.2 Dissection of eIF3 subunits´ functions

The general role of eIF3 in the cell is to act as the protein scaffold for the formation of initiation complexes. Its strategic location on the small ribosomal subunit enables it to bridge different components of the PIC and, moreover, to participate also in the initiation process itself by influencing mRNA scanning and start codon recognition (Hinnebusch, 2006). So far, mainly extensive genetic and biochemical studies in budding yeast have provided the insight into the function of eIF3 core subunits. But with ever-growing improvements in the resolution of cryo-

EM reconstructions together with cross-linking, mass spectrometry and integrative structure modelling, several models of the partial PICs are now available allowing us to predict the roles of individual subunits by interconnecting our knowledge from the functional assays with the subunits positions on the 40S ribosome (Aylett et al., 2015; Erzberger et al., 2014; Hashem et al., 2013; Hussain et al., 2014; Llácer et al., 2015).

Taking all available structural information into account, Erzberger et al. presented a model of molecular architecture of yeast and also mammalian eIF3•eIF1•40S complex (Fig. 2.3 A) (Erzberger et al., 2014). Consensus positions of conserved eIF3 subunits match in yeast and mammalian model and are also consistent with the collected biochemical and genetic data. Mammalian eIF3 octameric core contacts only relatively small area of the solvent-exposed region of 40S subunit near the mRNA exit channel mainly by its head (eIF3c) and left arm (eIF3a) with the rest of octameric subunits pointing outwards (Fig. 2.3 B). On the other hand, the eIF3bgi subcomplex resides on the opposite end of mRNA channel and is contacted by the CTD of eIF3a. Another important observation is that the NTD of eIF3c may extend across the subunit interface surprisingly from the ribosomal E-site and interact with its binding partners eIF1, eIF5 and TC possibly coordinating their functions (Karásková et al., 2012). These findings are consistent also with the very recent structures provided by two other research groups (Aylett et al., 2015; Llácer et al., 2015).

The previously reported position of the left leg of eIF3 consisting of subunits eIF3f and m in the 40S•eIF3•IRES complex was proposed to finally explain the observed eIF3 ribosomal anti-association activity that prevents the premature 40S-60S joining as it seemed to occlude some of the known intersubunit bridging contacts (Siridechadilok et al., 2005). However, in the newer model, the orientation of eIF3 on the 40S subunit is different (Hashem et al., 2013), which could be due to a possibility that eIF3 might bind to the 40S subunit in a different manner when the internal ribosome entry site (IRES) element is present. While the left leg in the newer model is rather sticking out to space not making any contacts with the ribosome, the tip of eIF3´s head could be actually responsible for the disruption of intersubunit bridge (Hashem et al., 2013).

Interfering with the factors residing near the mRNA entry channel such as eIF3a-CTD, eIF3b-RRM and eIF3j impairs the mRNA recruitment and affects the start codon selection (Chiu et al., 2010). As for the eIF3g and eIF3i, which were previously reported as redundant for the 43S PIC formation (Masutani et al., 2007), they were actually implicated in the scanning process (Cuchalová et al., 2010).

Little is known about the function of non-core eIF3 subunits. Essential conserved subunits could be required for the global protein synthesis whereas non-essential subunits could for example modulate the mRNA specificity. The aforementioned two distinct eIF3 complexes of fission yeast that comprise overlapping set of core subunits but are distinguished by the presence of PCI-containing protein eIF3m and MPN protein eIF3h or non-essential PCI protein eIF3e and its module ii partner eIF3d were shown to be associated with different sets of mRNA, with eIF3e complex being associated with more restricted set than eIF3m-containig complex (Zhou et al., 2005). Another case of translational regulation by an eIF3 subunit was found to act during zebrafish embryogenesis, when one isoform of eIF3h was shown to target the cohort of lens-associated crystallin isoform mRNAs to polysomes and complementary to this, its depletion caused defects in the development of brain and eyes (Choudhuri et al., 2013). The most recent study, which conducted genome-wide search for human transcripts directly bound to eIF3 found that four eIF3 subunits, namely eIF3a, b, d and g, directly crosslinked to RNA (Lee et al., 2015). Detected interactions were subunit and mRNA specific and mapped predominantly to conserved stem-loop structures in the 5´ UTR of transcripts, which strengthens the proposal of the transcript-specific engagement of eIF3 in translational control. However, the most surprising outcome of this research was, that eIF3 acted as both, a translational activator and repressor, depending on the specific cellular mRNAs. Finally, individual overexpression or underexpression of eIF3 subunits has been observed in specific cancers, which would suggest for example their role in the regulation of cellular proliferation (for a review see Hershey, 2014).

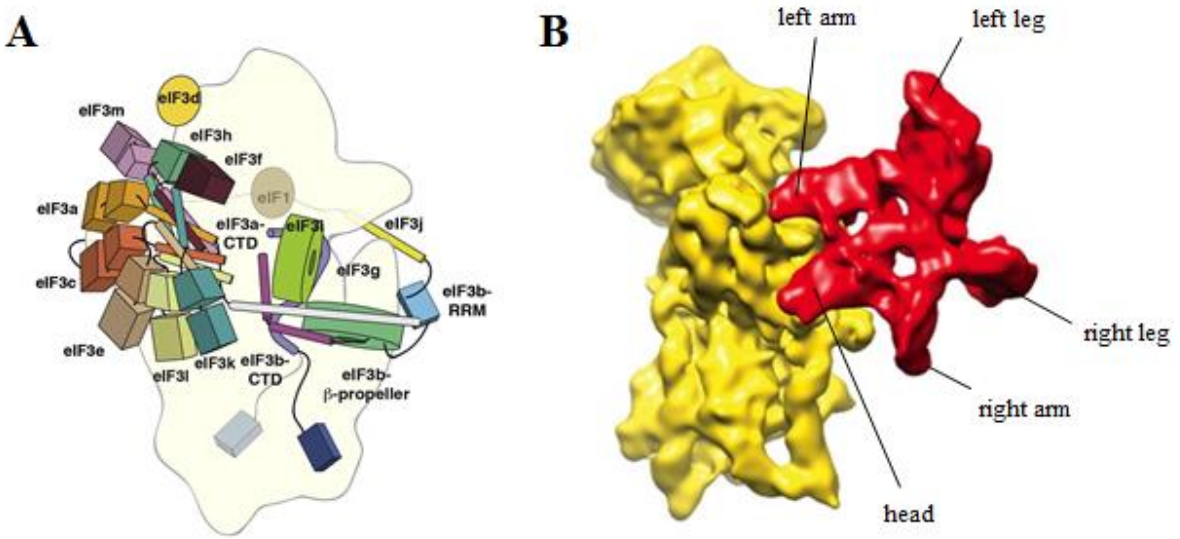

Figure 2.3 Schematic illustration of mammalian eIF3 on the 40S subunit from the ribosome solvent-exposed site (A) and its rotated cryo-EM structure (B) (pictures were adapted from Erzberger et al., 2014).

2.3 eIF3e

The e subunit of eIF3 was first denoted as an integration site 6 protein (INT6) since its gene locus was shown to be a preferred chromosomal insertion site of mouse mammary tumour virus (Miyazaki et al., 1995). Later on, this 48-kDa protein was found to be associated with 40S ribosomes and to co-purify with other eIF3 subunits in fission yeast (Akiyoshi et al., 2001). Even though the genome of budding yeast does not encode for eIF3e, it is quite conserved among other eukaryotes and several defects in mutant fission yeast can be rescued by its human ortholog (Bandyopadhyay et al., 2000).

In mammals, eIF3e is a part of the eIF3 structural octameric core making up its right arm (Querol-Audi et al., 2013). Although its precise interactions with other eIF3 subunits are not known, in the proposed connection map eIF3e makes contacts with eIF3d and l, and probably also with eIF3c and one or more module i subunits (Zhou et al., 2008). It was also shown that together with eIF3c and d it directly interacts with eIF4G, thereby helping in the recruitment of the 40S subunit to capped mRNAs (Villa et al., 2013; Walsh & Mohr, 2014). In addition, eIF3e promotes the binding of MAPK signal integrating kinase 1 (Mnk1) to eIF4G, which enables the phosphorylation of eIF4E that is necessary for the regulation of translation of specific mRNAs (Walsh & Mohr, 2014).

Several lines of evidence suggest that eIF3e has a function in influencing cell´s proteome composition by being engaged also in other pathways besides translation. Silencing eIF3e by RNA interference strongly impairs nonsense-mediated mRNA decay pathway (NMD) that is responsible for the degradation of transcripts with premature termination codon (Morris et al., 2007). Moreover, eIF3e was shown to interact with subunits of 26S proteasome (Hoareau Alves et al., 2002) and consistent with this finding, deletion of eIF3e in fission yeast affects proteasome activity resulting in the accumulation of polyubiquitinated proteins (Yen et al., 2003).

The role of eIF3e in the context of translation was mostly studied in *S. pombe*. eIF3e knock-out strains are viable, show slow growth phenotype but the rates of translation initiation are only moderately reduced even though eIF3 was found to be unstable (Akiyoshi et al., 2001; Bandyopadhyay et al., 2000; Bandyopadhyay et al., 2002). Similar effect of decreased cell proliferation was observed also in human glioblastoma cells upon eIF3e siRNA knock-down (Sesen et al., 2014). However, the importance of this subunit for the integrity and function of human eIF3 *in vivo* has not been systematically investigated yet.

Aims of the Thesis

As already stated in the Introduction, human eIF3 is a lot less explored complex than its budding yeast homolog. In our previous work, we have shown that downregulation of eIF3a and c subunits had a dramatic effect on the integrity of eIF3 in HeLa as well as in HEK293 cells. It also negatively affected cell proliferation and impaired translation in both cell lines. Thus, the aim of my work has been to continue in the previously established pipeline of our research group to systematically tackle each subunit of human eIF3 by means of its siRNA-mediated silencing followed by biochemical and functional analysis of its consequences.

In this study, I focus on the eIF3e subunit and explore the effects of its knock-down in HeLa cells to find out, if the depletion of this subunit affects:

i) protein or mRNA levels of other eIF3 subunits

ii) integrity of eIF3

iii) cell proliferation

iv) translational rates

v) and binding of eIF3 to 40S subunit

It would be interesting to compare the consequences of the eIF3e depletion in the HeLa cell line with those reported from other human cell lines and also fission yeast to see if they are similar and if the role of this subunit is equally important for the cell in lower and higher eukaryotes.

Materials and Methods

3 Materials

All plastic culture vessels were purchased from the company TPP Techno Plastic Products®

4 Chemicals

Dulbecco´s Modified Eagle´s medium (DMEM) (Sigma-Aldrich®)
Foetal Bovine Serum (FBS) (Sigma-Aldrich®)
1x Phosphate-Buffered Saline (PBS) for cell cultures (supplied by core facility of IMG, AS CR)
Trypsin (2.5%), no phenol red (Life Technologies)
ON-TARGETplus Human EIF3E (3646) siRNA SMARTpool (Dharmacon/GE, cat # L-010518-00-0005)
ON-TARGETplus Non-targeting siRNA #3 (Dharmacon, cat # D-001810 03-05)
INTERFERin® (Polyplus transfection™)
Complete EDTA-free tablets (Roche)
Cycloheximide (Sigma-Aldrich®)
HEPES (Sigma-Aldrich®)
$MgCl_2$ (Serva)
KCl (Chemapol)
PMSF (Serva)
Aprotinin (Serva)
Pepstatin (Serva)
Leupeptin (Serva)
NaF (Fluka Analytical®)
DTT (Serva)
Tris (Serva)
Triton X-100 (Sigma-Aldrich®)
Tween®20 (Sigma-Aldrich®)

SDS (Serva)
Glycine (Serva)
NaCl (Lach-ner)
BSA (NEB®)
Bio-Rad Protein Assay reagent (Bio-Rad)
β-mercaptoethanol (Sigma-Aldrich®)
Methanol (Lach-ner)
Instant fat-free dry milk (Nestle)
SuperSignal® West Femto Maximum Sensitivity Substrate (Thermo Scientific)
Chloroform (Lach-ner)
Isopropanol (Lach-ner)
RNA Blue Reagent (Top-Bio s.r.o.)
RNase-free water (Thermo Scientific)
DNase I buffer (10x) (NEB®)
DNase I (NEB®)
Maxima™ SYBR Green qPCR Master Mix (Thermo Scientific)
GammaBind™ G Sepharose™ beads (GE Healthcare)
Igepal® CA-630 (Sigma-Aldrich®)
HCl (Lach-ner)
MTT Reagent (Sigma-Aldrich®)

5 Solutions

Lysis buffer A: 20 mM Tris-HCl [pH 7.5], 50 mM KCl, 10 mM $MgCl_2$, 8.5 mM NaF, 1 mM DTT, 10 mM PMSF, 1 μg/ml aprotinin, 1 μg/ml leupeptin, 1 μg/ml pepstatin, 1 Mini Complete EDTA-free tablet/5 ml, 1% Triton X-100 (w/v)

Lysis buffer B: 20 mM Tris-HCl [pH 7.5], 50 mM KCl, 10 mM $MgCl_2$, 8.5 mM NaF, 1 mM DTT, 10 mM PMSF, 1 μg/ml aprotinin, 1 μg/ml leupeptin, 1 μg/ml pepstatin, 1 Mini Complete EDTA-free tablet/5 ml, 1% Triton X-100 (w/v), 5 mg/ml cycloheximide

Lysis buffer C: 10 mM HEPES [pH 7.5], 62.5 mM KCl, 2.5 mM $MgCl_2$, 8.5 mM NaF, 1 mM DTT, 10 mM PMSF, 1 µg/ml aprotinin, 1 µg/ml leupeptin, 1 µg/ml pepstatin, 1 Mini Complete EDTA-free tablet/5 ml, 1% Triton X-100 (w/v)

SDS-PAGE running gel: 25 mM Tris, 190 mM Glycine, 0.1 % SDS (w/v)

TBS: 20 mM Tris, 500 mM NaCl

TBS-T buffer: 20 mM Tris, 500 mM NaCl, 0.1 % Tween 20 (v/v)

SDS loading buffer (6x) : 60 % glycerol (v/v), 8 % SDS (w/v), 0.375 M Tris-HCl, 1.5 % β-mercaptoethanol (v/v)

blotting buffer: 25 mM Tris, 190 mM Glycine, 20 % methanol (v/v)

blocking buffer: 5 % instant fat-free dry milk in TBS-T

wash buffer A: 20 mM Tris-HCl [pH 7.5], 50 mM KCl, 10 mM $MgCl_2$

5 % sucrose buffer: 20 mM Tris-HCl [pH 7.5], 50 mM KCl, 10 mM $MgCl_2$, 5 % sucrose (w/w), 1 mM DTT

45 % sucrose buffer: 20 mM Tris-HCl [pH 7.5], 50 mM KCl, 10 mM $MgCl_2$, 45 % sucrose (w/w), 1 mM DTT,

7.5 % sucrose buffer: 10 mM HEPES [pH 7.5], 62.5 mM KCl, 2.5 mM $MgCl_2$, 7.5 % sucrose (w/w), 1 mM DTT

30 % sucrose buffer: 10 mM HEPES [pH 7.5], 62.5 mM KCl, 2.5 mM $MgCl_2$, 30 % sucrose (w/w), 1 mM DTT, 0.075 % formaldehyde (v/v)

MTT solvent: isopropanol, 0.1 % Igepal, 4 mM HCl

6 Oligonucleotides

Name	Sequence (5´ - 3´)
eIF3c Fw	ATAGGATCCATATGTCGCGGTTTTTCACC
eIF3c Rv	TAAGTCGACGCTCAGTAGGCCGTCTGAG
eIF3d Fw	ATAGGATCCATATGGCAAAGTTCATGAC
eIF3d Rv	TAAGTCGACGCTTAAGTTTCTTCCTCTTC
eIF3e Fw	ATAGGATCCATATGGCGGAGTACGACTTG
eIF3e Rv	TAAGTCGACGCTCAGTAGAAGCCAGAATC
eIF3k Fw	TACGGATCCAGATGGCGATGTTTGAG
eIF3k Rv	TAAGTCGACTATTACTGGGAGGAGGC
eIF3l Fw	ATAGGATCCATATGTCTTATCCCGCTG
eIF3l Rv	TAAGTCGACGCTCAAGGTCTCTGTCCC
β2-microglobulin Fw	GTATGCCTGCCGTGTGAACCATG
β2-microglobulin Rv	CAAATGCGGCATCTTCAAACCTCC

7 Antibodies

Primary antibodies:

Anti-eIF3a (Cell Signalling Technology®)

Anti-eIF3b, for Western blotting, rabbit polyclonal (Santa Cruz Biotechnology®, inc.)

Anti-eIF3b, for coimmunoprecipitation, goat polyclonal (Santa Cruz Biotechnology®, inc.)

Anti-eIF3c (Santa Cruz Biotechnology®, inc.)

Anti-eIF3d (obtained from Dr. Hiroaki Imataka, University of Hyogo)

Anti-eIF3e (abcam®)

Anti-eIF3f (obtained from Dr. Hiroaki Imataka, University of Hyogo)

Anti-eIF3g (obtained from Dr. Hiroaki Imataka, University of Hyogo)

Anti-eIF3h (Cell Signalling Technology®)

Anti-eIF3i (Sigma-Aldrich®)

Anti-eIF3j (Santa Cruz Biotechnology®, inc.)

Anti-eIF3k (abcam®)

Anti-eIF3l (obtained from Dr. Hiroaki Imataka, University of Hyogo)

Anti-eIF3m (Sigma-Aldrich®)

Anti-RPS14 (Santa Cruz Biotechnology®, inc.)

Anti-eIF2α (Santa Cruz Biotechnology®, inc.)

Anti-α-tubulin (Sigma-Aldrich®)

Secondary antibodies:

ECL™ Anti-mouse IgG, horseraddish peroxidase linked whole antibody (from sheep) (GE Healthcare)

ECL™ Anti-rabbit IgG, horseraddish peroxidase linked whole antibody (from donkey) (GE Healthcare)

8 Methods

8.1 Maintaning HeLa cell line

The HeLa cell line is probably the most widely used human model cell line in biological research. It is an epithelial culture cell line which was derived from the cervical carcinoma of a patient Henrietta Lacks (Gey et al., 1952).

The HeLa cells were cultured at 37ºC with 5 % CO_2 in Dulbecco´s Modified Eagle´s Medium (DMEM) containing 10 % foetal bovine serum (FBS). Cells were routinely split in 75 cm^2 culture flasks at ~ 80 % confluency (log phase) as follows. Used medium was removed from the culture vessel and cells were washed once with the pre-warmed 1x phosphate-buffered saline (PBS) (10 ml for 75 cm^2 cultivation flask). For the detachment of the cells, PBS containing 0.25 % (w/v) Trypsin (2 ml for 75 cm^2 of cultivation area) was added to the flask and incubated for 5 min at 37ºC. To enhance the detachment after incubation, flask was tapped and cells were then transferred to the 50 ml falcon tube with the pre-warmed DMEM + 10 % FBS to inactivate trypsinization. To determine the concentration of thus obtained cell suspension, 10 µl of cell suspension were loaded under the coverslip of the Bürker chamber (Marienfeld superior, cat # 0640030) and cells were counted in 4 squares. Final concentration of cells was calculated by following formula:

counted area: 4 squares (4 x 1 mm^2) = 4 mm^2

chamber depth: 0.1 mm

$$cell\ concentration = \frac{counted\ cells}{4\ mm^2\ \times\ 0.1\ mm} \times 10{,}000\ [cells/ml]$$

Cells were seeded to the desired density (1 million cells/75 cm^2 cultivation flask) and cultured in 20 ml of DMEM + 10 % FBS under the aforementioned conditions.

All work done with HeLa cell lines until their processing for individual assays was done in sterile conditions.

8.2 siRNA transfection of HeLa cells

RNA interference (RNAi) is a broadly used method to specifically silence the expression of a desired gene. Its robustness strongly relies on several factors, such as a type of the siRNA delivery, transfection reagents and their concentrations, culturing conditions, exposure time of siRNA to cells or targeted model system (cell type or whole organism).

In this study, we employed transient siRNA transfection of HeLa cells by means of a lipofection. Lipofection is based on the principle, that negatively charged nucleic acids are packaged into lipophilic particles, which facilitate the cellular uptake of siRNA through their fusion with the membrane lipid bilayer of cell.

For transfections, cells were seeded to either Ø 15cm culture dishes (1.4 million cells further treated with non-targeting siRNA or 1.8 million cells further treated with siRNA against eIF3e in 20 ml of DMEM + 10 % FBS) or to 24-well plates (14,000 cells/well for control and 18,000 cells/well for eIF3e knock-down in 500 µl of DMEM + 10 % FBS) and were cultured under the standard conditions mentioned above. The difference in the number of seeded cells treated with different siRNAs is due to the initial observations that the proliferation of cells treated with siRNA against eIF3e is decreased, thus to obtain enough biological material for experiments we decided to start with more cells in case of eIF3e knock-down. These initial observations were later confirmed by MTT assay (see Results Fig. 10.1). Used culture vessels depended on further experimental procedure. 24 h after seeding, cells were transfected with ON-TARGETplus siRNA SMART pool system (either with non-targeting siRNA or siRNA against human eIF3e). For all experiments, cells were transfected with the final concentration of 5 nM of a given siRNA. As a transfection reagent was used INTERFERin® and its volume was adjusted according to the culture vessel format, volume of complete medium and used siRNA concentration (3 µl/well of 24-well plate, 100 µl/Ø15 cm dish).

Transfection procedure by itself was done as follows. Respective siRNA was diluted into DMEM without FBS in a manner to reach the concentration of 5 nM in the final volume of medium in which the cells are cultured taking into account also the volume of added transfecting cocktail (concrete volumes for culture vessels are specified in Tab 1). After resuspending of siRNA in DMEM, INTEREFERin® was added, mixture was mixed and then

incubated for 10 minutes at room temperature (RT) to allow the complexation reaction of siRNA into lipophilic particles. Transfection mix was added to the cells and homogenized by gentle swirling of the cultivation vessel. Cells were then incubated under standard conditions until their processing for individual experiments.

Tab 1. Summarizing table of transfection conditions for HeLa cells

Type of a vessel	**Number of cells to seed**	**Volume of medium to culture the cells in [ml]**	**Transfection mix components**		
			Volume of INTERFERin® [µl]	**Volume of DMEM for complexation [ml]**	**Final siRNA concentration [nM]**
24-well plate	14,000 or 18,000	0.5	3	0.1	5
Ø15 cm dish	1.4 or 1.8 x 10^6	20	100	2	5

8.3 Whole-cell extract (WCE) preparation

Cells were harvested 72h posttransfection (~ 80 % confluence). Whole procedure was done either on ice or in the cold room (4ºC). First, the medium was aspirated and cells were rinsed twice with cold 1x PBS (10 ml for Ø15 cm dish). Cells were lysed directly on the plate by adding ice-cold lysis buffer (600 µl for Ø15 cm dish, 30 µl/well of 24-well plate), collected by scraping to one area of plate, re-pippeted several times to allow their dissociation and transferred to pre-cooled microcentrifuge tube. Cell lysate was then incubated for 5 minutes on ice and vortexed few times in between to ensure the complete lysis. Lysate was cleared by centrifugation at 15,500 g, 4ºC for 5 min. Supernatant was transferred to a new tube and processed directly or deep-froze in liquid nitrogen and maintained at - 80ºC.

8.4 Bio-Rad protein assay

Bio-Rad protein assay was used to measure total protein concentration in solution. The method is based on the Bradford assay, when Coomassie Brilliant Blue G-250 dye changes the colour upon binding to proteins which causes a shift in the absorbance of a dye from 495 nm to 595 nm.

The standard curve has been calibrated using measurements of serial dilutions of bovine serum albumin (BSA) at known concentration. Absorbance was measured in Beckman Coulter™ DU® 530.

Protein concentration of the samples was calculated as a mean of 3 different dilution measurements (0.5 µl, 1 µl or 2 µl of a sample/1 ml Bio-Rad protein assay reagent).

8.5 SDS-PAGE

Protein samples were diluted in the 6x SDS loading buffer to a final sample buffer concentration of 1x, boiled for 5 – 10 minutes at 95ºC and loaded to the gel in equal amounts. All samples were separated in 4 – 20 % gradient gels (Criterion™ TGX™ Precast Gels; Bio-rad). As a protein marker was used Precision Plus Protein™ Standards Dual Color (Bio-Rad). Samples were run under denaturing conditions of SDS-PAGE running buffer at 200 V for 40 min.

8.6 Western blotting

Proteins are transferred from the gel and immobilized to nitrocellulose membrane (blotting). Gel is assembled to the transfer sandwich in the presence of pre-cooled transfer buffer in the following order: Wattman filter paper, gel, nitrocellulose membrane and Wattman filter paper. Transfer sandwich is positioned in between two sponges soaked also in the blotting buffer and put between cathode and anode (the blot should be on the anode and gel on the cathode) in the transfer tank (Criterion™ cell; Bio-Rad). The tank is filled with the blotting buffer and blotting procedure is run at 25 V (constant current should not exceed 2 A) for 1.5 hour in the cold room. After blotting, membrane is incubated at RT for 1 hour, gently shaking in blocking buffer to saturate unoccupied protein-binding sites on the membrane to prevent nonspecific binding of antibodies. In the case of immunoblotting for different proteins, membrane is cut and individual strips are then probed overnight with specific primary antibodies diluted in 5 % milk, 1x TBS, 0.1 % Tween®20 against the protein of interest in the cold room, gently shaking. Next day, the blot is rinsed with TBS-T (2 x 10 min) and then incubated with the horseradish peroxidase-conjugated secondary antibody solution for 1 hour

at RT, gently shaking. The blot is then again rinsed with TBS-T (2 x 10 min) and labelled protein bands are visualized by chemiluminiscent detection.

8.7 Chemiluminiscent detection and data analysis

As a chemiluminiscent substrate was used SuperSignal® West Femto Maximum Sensitivity Substrate. Working solution was prepared by mixing Luminol/Enhancer with Stable Peroxide Buffer in 1:1 ratio (2 ml of detection reagent is sufficient for) and applied on membrane to cover the whole surface. After 1 minute of incubation, excess of the reagent was removed and the chemiluminiscent signal was captured using different exposure times (1s, 4s, 5s, 10s, 40s, 1 min, 3 min, 5 min and 10 min) in G:BOX iChemi device.

As an image analysis software to read the band intensity of detected proteins and concentration analysis was used QuantityOne® 1-D Analysis software.

8.8 RNA isolation

During the process of RNA isolation, gloves, RNase-free solutions and sterile plastic ware were used to avoid RNA degradation.

Cells were grown in 24-well plate, transfected 24 h after the seeding as described previously and RNA isolation was done 72 h posttransfection. After aspirating the medium, cells were lysed directly in the wells with RNA Blue Reagent (250 µl/well), homogenized by pipetting and transferred into 1.5 ml tube. Lysates were incubated for 5 min at RT to permit complete dissociation of nucleoprotein complexes. After that, chloroform was added (200 µl per 1 ml of RNA Blue Reagent used for lysis), tubes were shaken vigorously for 15 s, incubated at RT for 3 min and finally centrifuged at 15,500 g for 5 min at 4ºC. The upper aqueous phase containing RNA was transferred to new 1.5 ml tube and RNA was precipitated by mixing with isopropanol (500 µl per 1 ml of RNA Blue Reagent used for initial lysis). Samples were incubated for 10 min at 4ºC and then centrifuged at 15,500 g for 15 min at 4ºC. After centrifugation, supernatant was carefully removed and RNA pellet was washed with 1ml of 75 % ethanol. Sample was mixed by vortexing and centrifuged at 15,500 g for 5 min at 4ºC. Ethanol was discarded and RNA pellet was air-dried at air. RNA was dissolved in 25 µl RNase-free water by passing it several times through a pipette tip and incubated for 10 min at 50ºC.

8.9 DNase I treatment

To remove possible contaminating genomic DNA, RNA samples were treated as follows. To the resuspended RNA pellets was added DNase I buffer (10x) to the final sample buffer concentration of 1x and 1 µl of DNase I. Samples were incubated at 37ºC for 1 h.

After DNase I digestion, RNA concentration and purity was assessed by UV spectroscopy.

8.10 Reverse transcription

For reverse transcription of total RNA to single-stranded cDNA was used High Capacity cDNA Reverse Transcription Kit (Applied Biosystems®).

Kit components:	10x RT Buffer 10x RT Random Primers 25x dNTP Mix (100 mM) MultiScribe™ Reverse Transcriptase, 50 U/µl RNase Inhibitor

For reverse transcription was used 700 ng of total RNA per 20 µl reaction.

First, 2x RT reaction mix was prepared on ice according to Tab 2.

Tab 2. Composition of 2x reverse transcription master mix.

Component	Volume/reaction [µl]
10x RT buffer	2.0
25x dNTP Mix (100 mM)	0.8
10x RT Random primers	2.0
MultiScribe™ Reverse Transcriptase	1.0
RNase Inhibitor	1.0
Nuclease-free water	3.2
Total per reaction	10

10 µl of 2x RT mix was pipetted into individual tubes and then 10 µl of RNA sample were added (700 ng). Reaction mix was pipetted up and down few times, tubes were shortly spun down and placed into the thermal cycler (Mastercycler® ep; Eppendorf). Thermal cycler was programmed according to Tab 3.

Tab 3. Thermal cycler conditions for reverse transcription.

	Step 1	Step 2	Step 3	Step 4
Temperature [ºC]	25	37	85	4
Time [min]	10	120	5	∞

8.11 Quantitative real-time PCR

SYBR Green based qPCR was used for determination of mRNA expression levels of module ii subunits (c, d, e, k and l). For detection of individual subunits was used a set of two primers (sequences of used oligonucleotides can be found in section 7 Oligonucleotides) that flank the target region. As a reference gene for relative normalization was used β2-microglobulin. As a negative control was used isolated RNA sample without DNase I treatment. Due to the sensitivity of qPCR method, each primer pair was used in three technical replicates and qPCR was performed also in biological triplicates (either of cDNA from control cells or eIF3e knocked-down cells).

Reaction mixes were prepared as follows. For each primer pair and cDNA solution was prepared a master mix with ready-to-use Maxima™ SYBR Green qPCR Master Mix (2x) and 10 µl reactions were distributed into 96-well plate. Components of qPCR reaction are listed in Tab 4. Thermal cycler was programmed according to the cycling conditions below.

Step	**Temperature [ºC]**	**Time**	**Number of cycles**
Initial denaturation	95	10 min	1
Denaturation	95	14 s	44
Primer annealing	58	21 s	
Extension	72	21 s	
Final extension	72	3 min	1
Melting curve analysis	65 – 90 increment	5 s	1

Data acquisition was performed during extension step.

Tab 4. Composition of 1x reaction mix for qPCR.

Component	Volume/reaction [µl]
cDNA	1
Primer Fw (100 µM)	0.2
Primer Rv (100 µM)	0.2
SYBR Green master mix (2x)	5
Nanopure H_2O	up to 10

8.12 Coimmunoprecipitation assay

Coimmunoprecipitation assay (CoIP) is used to study protein-protein interactions *in vivo*. To perform CoIP, first antibody against the target protein (in this case eIF3b) is bound to Sepharose beads covered with protein G and then complexes containing the target protein (human eIF3 complex) can be coimmunoprecipitated with the target protein via its binding with antibody-coupled beads.

Cells were grown in Ø15 cm dish and harvested with lysis buffer A 72 hours posttransfection. GammaBind™ G Sepharose™ beads were washed 3 times with wash buffer A as follows. For each wash, to 100 µl of beads were added 1 ml of wash buffer A, solution was centrifuged at 300 g for 2 min at 4ºC and supernatant was removed. After final wash the same volume of wash buffer A as was the volume of beads was added to the beads to create 50 % slurry. Beads were then pre-incubated with anti-eIF3b (3 µg of antibody/100 µl 50 % slurry) on rotating shaker at 4ºC for 2 hours. As a negative control was used 50 % slurry without pre-incubation treatment with antibody. Beads were then washed once with wash buffer A to get rid of excess of antibody and again 50 % slurry was made. To 40 µl of 50 % slurry was added 1 mg of total proteins of the WCE diluted in wash buffer A so the final concentration of Triton X-100 does not exceed 0.3 % to prevent intervening with immunoprecipitation. Mixture was incubated overnight at 4 ºC on rotating shaker. From each WCE used for CoIP was also prepared 5 % input sample (if for CoIP was used 1 mg of WCE, then 5 % input means diluting 50 µg of WCE in washing buffer A and boiling at 95ºC for 5 min with SDS loading buffer to its final concentration in the sample of 1x). Next day, beads were washed 4 times with washing buffer A + 0.2 % Triton X-100 to remove non-specific binding. Last wash was done with washing buffer A without Triton X-100. From the first wash fraction was taken 5 % of supernatant to which was added SDS loading buffer to its final concentration in the sample of 1x and boiled at 95ºC for 5 min. Coimmunoprecipitated proteins were eluted in SDS loading

buffer by boiling for 10 min at 95ºC and eluates were analysed by SDS-PAGE and subsequent Western blotting.

8.13 Polysome profile analysis

Polysome profile analysis is a method used to assess efficiency of translation in cells. Linear sucrose gradients are used for the velocity separation of mRNAs bound to multiple ribosomes known as polysomes from mRNA bound to a single ribosome also called monosome. Increase in translation initiation rates is determined by more frequent loading of ribosomes on mRNA and thus global translation level can be defined as the ratio of polysomes to monosomes (P/M ratio). In theory, it drops in case of some translation initiation defects. Schematic of the method is represented in Fig. 8.1

Cells were grown in Ø15 cm dish and 3 days after transfection, cycloheximide was added to the cells to final concentration of 100 µg/ml and cells were incubated for 5 min at 37ºC prior to their harvest with lysis buffer B. Purpose of the cycloheximide is to freeze ribosomes on mRNA.

5 – 45 % linear sucrose gradients were prepared as follows. To the bottom of polyallomer centrifuge tube (Beckman Coulter®) was added 6 ml of 45 % sucrose buffer and on top of it carefully 6 ml of 5 % sucrose buffer followed by mixing the two layers in the capped tube using a Gradient $Master_{ip}$ (Biocomp).

On top of the sucrose gradients were slowly loaded at least 10 A_{260} units of WCE. Additional lysis buffer can be used to assure that the gradients are loaded with an equal volume due to maintaining the balance during centrifugation. Tubes were then put into the rotor buckets which were hung onto the strings of the swinging bucket rotor (SW41Ti, Beckman) and gradients were centrifuged at 39,000 rpm for 2.5 h at 4ºC.

Polysome profile was analysed by using a pump syringe apparatus (Brandel) attached to the UV spectrophotometer (Type 11 Optical Unit, Teledyne Isco) which was connected to the chart recorder (UV-6 detector, Teledyne Isco). After spinning, tube was placed on the tube piercer and the bottom was punctured with the needle to allow flow of the 60 % sucrose. Once the sample reaches the UV detector (A_{254}), pen will record the peak of the free material followed by 40S ribosomes and continuing through polysome complexes. To calculate the P/M ratio, the area under the curve of 80S peak and polysomes curve was quantified by Engauge software.

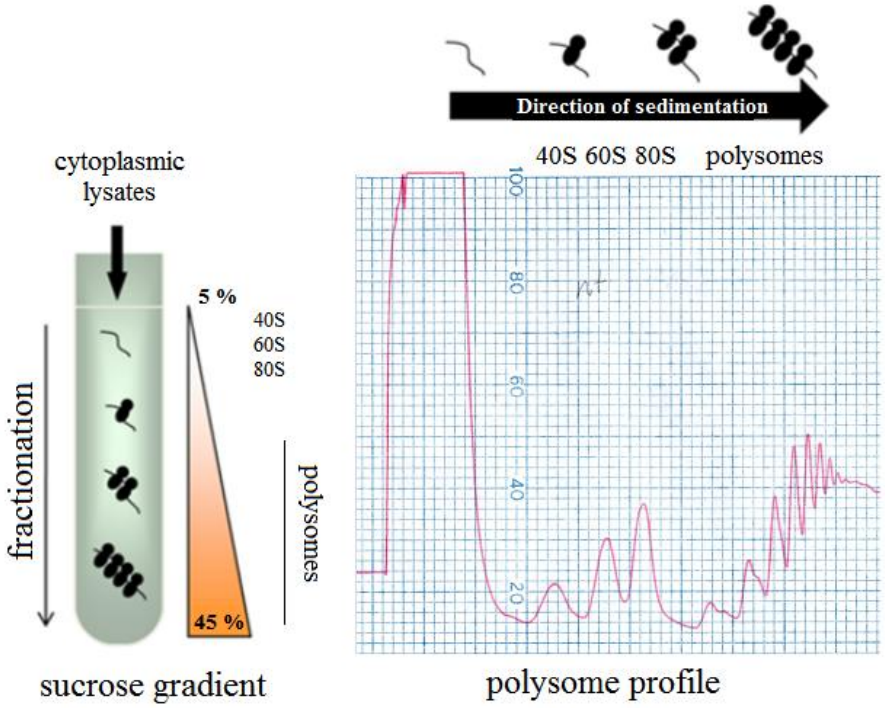

Figure 8.1 Schematic representation of polysome profiling. On the left is depicted formation of 5 – 45 % sucrose gradient and on the right is shown recorded polysome profile with indicated ribosomal species (figure was adapted and modified for this theses purpose from Abdelmohsen, 2012).

8.14 40S binding assay

Analysis of the composition of 43-48S ribosomal complexes utilizes isolation of these complexes from WCE using density sucrose gradient fractionation followed by Western blotting to detect individual components (in this case presence of human eIF3 complex subunits).

Cells were grown in Ø15 cm dish and were harvested 3 days after transfection with lysis buffer C. 7.5 – 30 % linear sucrose gradients were prepared in the same manner as 7.5 – 30 % gradient described for polysome analysis. However, 30 % sucrose buffer contains 0.075 % formaldehyde to crosslink proteins within supramolecular complexes to prevent their dissociation during high velocity sedimentation. On top of the gradient were loaded 10 - 14 A_{260} units of WCE and additional lysis buffer was used to assure that the gradients are loaded with an equal volume due to maintaining the balance during centrifugation. Tubes were then put into the rotor buckets which were hung onto the strings of the swinging bucket rotor (SW41Ti, Beckman) and gradients were centrifuged at 22,200 rpm for 17 h at 4ºC. Limitation of this method is that some weaker interactions may not survive centrifugation, preventing them

to be scored in this assay. Therefore, we lowered speed and increased the time of centrifugation as opposed to conditions used in previous work (Wagner et al., 2014).

After spinning, tube was placed on the tube piercer and the bottom was punctured with the needle to allow flow of the 60 % sucrose. ~ 600 µl fractions were collected and polysome profile was recorded to later determine the fractions containing 40S ribosomal subunits for further processing. Fractions were precipitated overnight at - 20ºC with 100 % cold ethanol. Next day, they were spun at 15,500 g, 4ºC for 30 min, supernatant was discarded and pellet was washed with 1 ml of 75 % ethanol. Samples were again spun at 15,500 g, 4ºC for 10 min, obtained pellets were dried and boiled at 95ºC in 1x SDS loading buffer to reverse cross-linking. Fractions were analysed by SDS-PAGE followed by Western blotting.

8.15 MTT assay

MTT (3-[4,5-dimethylthiazol-2-yl]-2,5 diphenyl tetrazolium bromide) assay is a standard calorimetric method to examine cell viability and proliferation. The yellow tetrazolium salt is reduced into formazan crystals by mitochondrial activity of living cells. The resulting purple formazan is solubilized and quantified by spectrophotometer at a certain wavelength (500 – 600 nm).

Cells were grown in 24-well plates (14,000 cells/well) and were transfected 24 hours after seeding. MTT solution was freshly prepared at 0.83 mg/ml of MTT reagent in DMEM + 10 % FBS. First, medium was aspirated from cells and 200 µl of MTT solution were added to each well, followed by 3.5 hour incubation at 37ºC. After that, MTT solution was removed and cells were carefully washed with 500 µl of 1x PBS. Formazan crystals were dissolved in 200 µl of MTT solvent and absorbance at 592 nm was recorded with reference wavelength of 620 nm in TECAN Sunrise™. A blank experiment for the detection of cell-free background absorbance was done in parallel by filling always one well only with media.

MTT assay was performed every day during 4 day period in pentaplicates, starting 24 hours after seeding with untransfected cells and continuing everyday with cells treated either with non-targeting siRNA or siRNA against eIF3e.

Results

9 Effect of siRNA-mediated knock-down of eIF3e on other human eIF3 subunits and eIF3 integrity

The siRNA knock-down technique is one of the ways how the function of a gene can be assessed (Elbashir et al., 2001). Similarly to the gene knock-out, it depletes the cell of its product, although not with 100 % efficiency as the gene it is still present in the genome and only its expression is post-transcriptionally silenced, leading to the reduced amounts of the protein of interest. In order to determine the significance of the eIF3e subunit, we took advantage of such approach and knocked-down its expression in the HeLa cell line (further denoted as $eIF3e^{K.D.}$). To be sure that any observed defects are not just side effects of a possible toxicity of a lipofection reagent or stress induced by a transfection procedure, we used as a reference the HeLa cells treated with non-targeting siRNA (NT).

Critical aspect of successful knock-down are transfection conditions. As shown previously, 5 nM concentration of targeting siRNA pool (ON-TARGETplus SMART pool siRNA system from Dharmacon/Thermoscientific) has proved to work very well in case of eIF3a and eIF3c knock-downs (further denoted as $eIF3a^{K.D.}$ and $eIF3c^{K.D.}$) (Wagner et al., 2014). For that reason, same concentration was used also for the downregulation of eIF3e subunit as well as for the control NT siRNA.

Cells were transfected 24 hours after their seeding. Two days later, used medium was replaced with a fresh one. Three days after transfection, cells were harvested, processed into a WCE that was subjected to the Western blot analysis to check the efficiency of the downregulation. As only transient siRNA transfection was employed, in a few generations the siRNAs are lost. But regularly, ~ 90 % reduction of the eIF3e protein content was achieved 72 hours posttransfection when compared to the eIF3e abundance in control cells (Fig. 9.1). As there are many factors, which can affect the visualized amount of a protein during Western blotting like loading or uneven transfer efficiency, the presented abundance of respective proteins was always calculated as their ratio to the loading control, which was in this case tubulin.

After the confirmation of effective downregulation of the e subunit, the remaining 12 eIF3 subunits were probed to monitor their protein levels (Fig. 9.1). Previous findings that

individual knock-downs of either eIF3a or c subunit have impact on protein levels of some other eIF3 subunits (in case of eIF3a$^{K.D.}$ all module ii and iii subunits, and in case of eIF3c$^{K.D.}$ only all module ii subunits), we were wondering if similar scenario will be also true for eIF3e$^{K.D.}$. Indeed, protein amount of 3 other subunits – eIF3d, k and l, all belonging to module ii, were dramatically reduced down to ~ 30 %. Unexpectedly, protein levels of the fifth module ii subunit, eIF3c, were not significantly reduced.

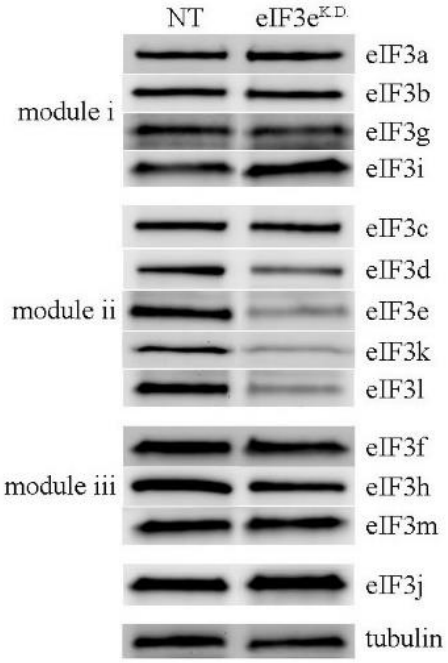

	eIF3e$^{K.D.}$
a	1.03 ± 0.18
b	1.17 ± 0.08
g	0.80 ± 0.10
i	1.22 ± 0.07
c	0.88 ± 0.20
d	0.26 ± 0.07
e	0.07 ± 0.03
k	0.35 ± 0.09
l	0.27 ± 0.13
f	1.0 ± 0.07
h	0.78 ± 0.12
m	0.89 ± 0.19
j	0.96 ± 0.15

Figure 9.1 Effect of siRNA-mediated downregulation of eIF3e subunit on protein levels of other 12 eIF3 subunits determined by the Western blot analysis. Western blots were quantified with QuantityOne programme and subunits' signals were normalized to tubulin. Values obtained from eIF3e$^{K.D.}$ cells are expressed relative to the values obtained from NT cells, which were set to 1. Standard deviations from at least 3 experiments are shown.

Next, we analyzed the mRNA levels of all module ii subunits to examine, if the decrease in their protein content could be the result of decreased transcriptional rates or mRNA degradation. For this purpose we performed qPCR using cDNAs converted from isolated RNAs that were obtained from cells 72 hours post-transfection. eIF3e was considered as a positive control, since its mRNA is expected to be cleaved and degraded by the action of targeting siRNA and eIF3c rather as a negative control, since its protein levels were not notably diminished and therefore also its mRNA levels were expected to be unchanged. Obtained data were quantified as the relative changes in the mRNA expression levels of subunits, in terms of C_q value, between eIF3e$^{K.D.}$ and control cells. Resulting ratios were normalized to β2-microglobulin (B2-MG) that served as a reference gene. qPCR showed that only mRNA levels of e subunit were decreased as the measurable signal from SYBRGreen comes ~ 6 cycles later.

The abundance of other subunits' mRNA was not affected. Similarly, it was previously shown that depletion of murine eIF3m subunit selectively decreases protein abundance of eIF3c, f and h subunits, but does not affect their mRNA levels (Zeng et al., 2013). Therefore, reduction of eIF3d, k and l protein levels can be attributed to either the repression of their mRNA translation or protein degradation.

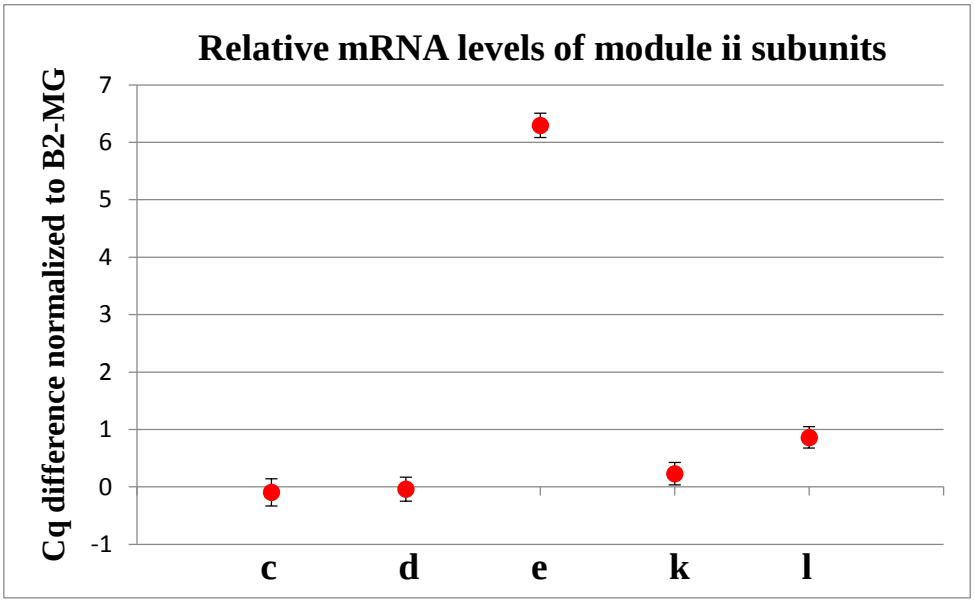

Figure 9.2 Effect of eIF3e knock-down on the mRNA levels of module ii subunits determined by qPCR 72 hours post-transfection. Depicted data points represent the difference in Cq values between eIF3$^{K.D.}$ and control cells. As a house-keeping gene for the normalization of measured mRNA levels was used B2-MG. Standard deviations are derived from three biological replicate for each subunit from either eIF3$^{K.D.}$ or control cells, with each biological replicate having also a technical triplicate.

Mass spectrometry has shown that the trimer composed of eIF3f, h and m subunits is connected with eIF3 through the interaction between eIF3c and h (Zhou et al., 2008). In eIF3c$^{K.D.}$, which led to the loss of all module ii subunits, only module i could be retrieved from WCEs using eIF3b as a bait in CoIP experiments (Wagner et al., 2014). Since eIF3e downregulation results in the reduction of protein levels of three eIF3 octameric core subunits (eIF3k, l and e itself) and one non-core subunit (eIF3d), but the protein levels of eIF3c and h subunits are not severely affected, it was interesting to ask, if the proposed interaction between these two subunits is strong enough to hold together modules i and iii. To answer this question, the integrity of eIF3 complex was examined by a CoIP. As a bait protein was used eIF3b since it was previously shown to pull-down the entire endogenous eIF3 from wild-type cells (Lee et al., 2015; Wagner et al., 2014).

CoIP experiments have revealed that only module i together with eIF3j can be sufficiently pulled-down via eIF3b when compared to the NT control (Fig. 9.3 with calculated

numbers in Fig. 9.4). Even though protein levels of eIF3c and module iii subunits are not affected by the eIF3e knock-down, they could not be retrieved with the same efficiency as from NT WCEs. eIF3c came down only with ~ 50 % efficiency with the rest of it existing perhaps free in the cytoplasm or linked to the module iii, however, the latter scenario should be further validated for example by another CoIP experiment using as a bait one of the module iii subunits. Module iii subunits came down also with a decreased efficiency (~ 55 %) and rather accumulated in the wash fractions, which can be possibly attributed to the missing eIF3c as a link and other module ii subunits.

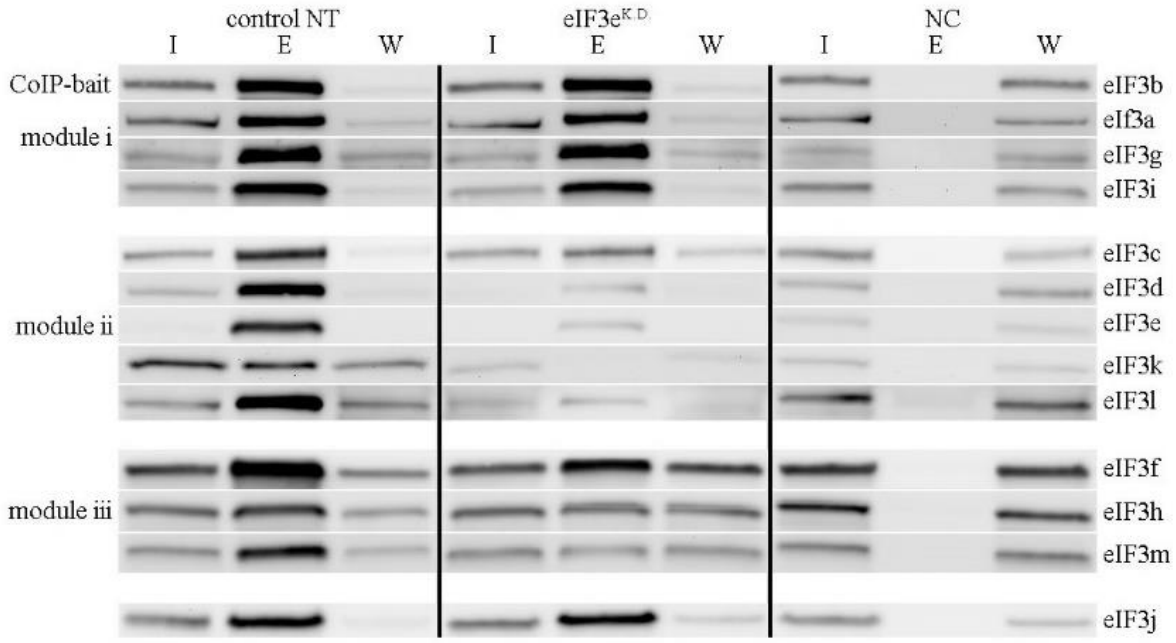

Figure 9.3 Effect of siRNA-mediated knock-down of eIF3e on the integrity of eIF3 complex determined by CoIP using eIF3b as a bait protein 72 hours post-transfection. Negative control (NC) was carried out using WCE from control cells and CoIP beads without antibody against eIF3b. I – input, E – eluate, W – wash.

module i	**eIF3e$^{K.D.}$**	module ii	**eIF3e$^{K.D.}$**	module iii + j	**eIF3e$^{K.D.}$**
a	0.88 ± 0.09	**c**	0.45 ± 0.25	**f**	0.66 ± 0.11
b	1.00	**d**	0.10 ± 0.07	**h**	0.59 ± 0.19
g	1.41 ± 0.13	**e**	0.10 ± 0.08	**m**	0.46 ± 0.20
i	1.02 ± 0.20	**k**	0.07 ± 0.06	**j**	1.26 ± 0.18
		l	0.07 ± 0.04		

Figure 9.4 Quantification of Western blot of coimmunoprecipitated proteins. Bands´ signals were quantified using programme QuantityOne and normalized to eIF3b. Values obtained with eIF3eK.D. cells are expressed relative to the values obtained with control cells, which were set to 1.00. Standard deviations from at least three individual experiments are given.

10 Viability and polysome profile analysis of eIF3e-depleted cells

Seeding the same number of cells for further treatment with either eIF3e targeting siRNA or NT siRNA repeatedly resulted in less WCE material obtained from eIF3e$^{K.D.}$ cells suggesting their impaired viability. To examine this, we employed a MTT assay. MTT is a yellow water-soluble dye that is converted by mitochondrial activity of living cells into purple formazan crystals. Water-insoluble crystalic formazan is further dissolved with MTT solvent containing non-ionic detergent (IGEPAL) and hydrochloric acid and the resulting colored solution can be quantified by measuring the absorbance at 595 nm.

The amount of generated formazan crystals reflects the metabolic activity of cells and is also proportional to the number of viable cells. Therefore, measuring the absorbance is a way how to quantify the change in the cell proliferation rate between control cells treated with NT siRNA and eIF3e$^{K.D.}$ cells. Cell viability was assessed daily after the transfection during a four day period, and the experiment was repeated three times. Protein levels of eIF3e were always checked by Western blot analysis to confirm the successful downregulation (data not shown).

The results of MTT assay showed a gradual decrease in cell proliferation and/or metabolic activity of HeLa cells treated with 5 nM concentration of anti-eIF3e siRNA when compared to NT siRNA-treated cells (Fig. 10.1). The most significant inhibition of cell proliferation (~ 80 %) was observed at the last recording day (Fig. 10.1 A). When looking at depicted growth curves, the first day after the transfection there is not a significant difference between compared cells (Fig. 10.1 B). Both samples exhibit slow linear growth, also known as lag phase, which can be attributed to the recovery from the seeding and transfection procedure. However, two days post-transfection, the difference is already detectable. As NT cells seem to enter into the exponential growth, also known as log phase, eIF3e$^{K.D.}$ cells continue in slow linear growth for another two days, when finally reaching plateau and subsequently stop proliferating. The short-coming of this assay is, however, that it does not detect apoptosis, in other words, it does not answer the question, whether the eIF3e depletion only slows down the cell growth and/or affects metabolic activity or if it leads to cell death.

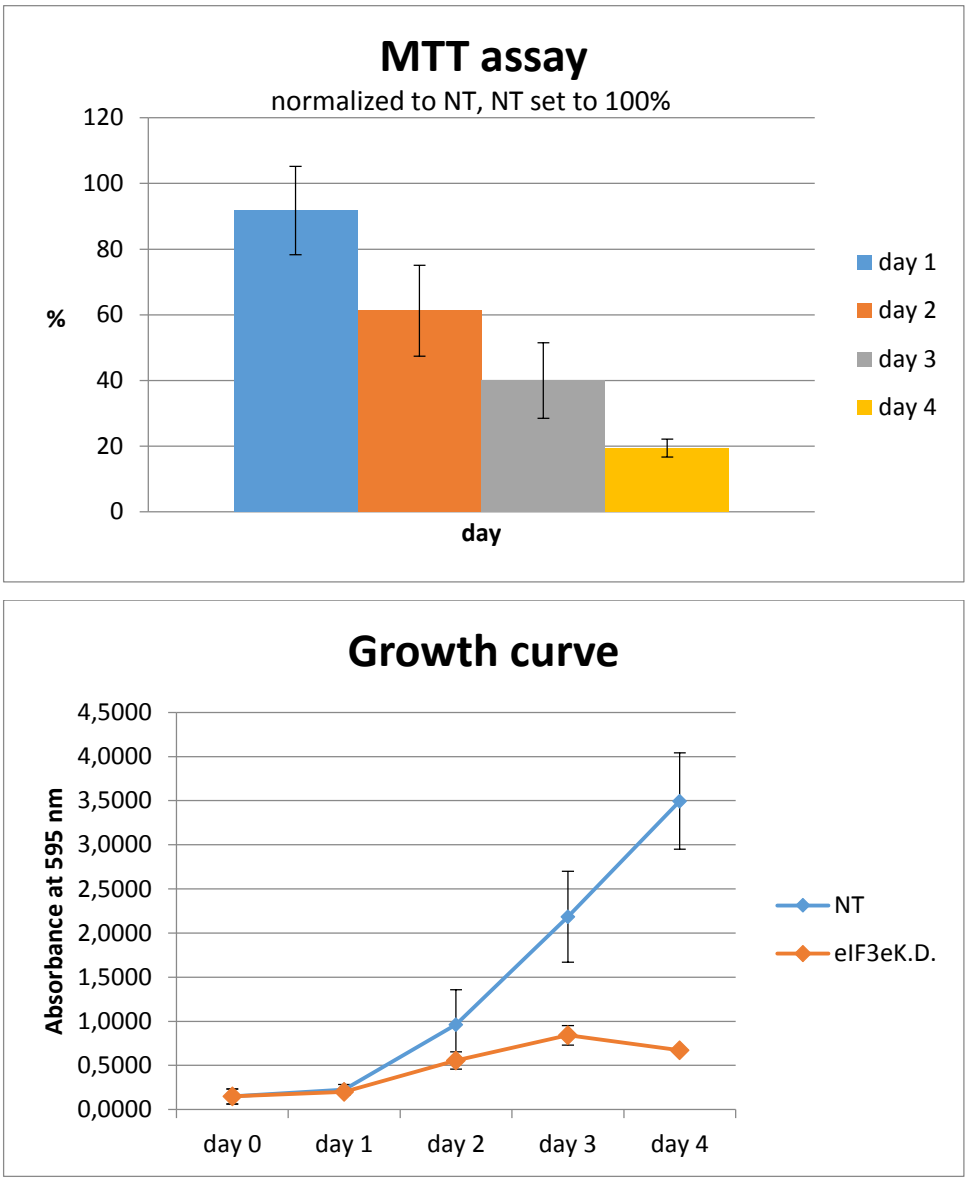

Figure 10.1 Effect of eIF3e downregulation on cell viability determined by MTT assay 24h, 46h, 72h and 96h post-transfection. In the bar graph representation of results, obtained values from eIF3e$^{K.D.}$ are normalized to those from NT control cells, which were set to 100 % (top). Growth curve was derived from the measured A595 units (bottom) and the points represent the mean of three independent experiments. Day 0 point represent the day of transfection, one day after seeding cells.

As eIF3e was shown to be a part of the molecular bridge that connects 40S subunit with mRNA, we examined if the observed cessation of cell proliferation could be due to impaired translation resulting from the depletion of this and other eIF3 subunits. Global translational rates were monitored by polysome profile analysis. This approach relies on the fact that more than one ribosome can be loaded on the same mRNA molecule leading to the formation of polysomes. To prevent their "run-off" from mRNAs during the WCE preparation, a drug cycloheximide was used to "freeze" them on mRNAs. The analysis itself is done by the separation of mRNA populations with different number of translating ribosomes in sucrose density gradient, which is subsequently analysed by measuring the absorbance at A_{254} and the

profile is recorded on the chart diagram. Translation initiation rates are then expressed as the ratio of polysomes to a single 80S peak – monosome, also known as the P/M ratio. Defects in translation initiation usually result in the decrease of this ratio due to the loss of polysomes and increase in the monosome peak representing mostly the run-off 80S couples since ribosomes are less efficient in loading of mRNAs.

In each experiment, ~ 10 A_{260} units of WCEs were loaded on top of the 5 – 45 % linear sucrose gradient followed by high velocity centrifugation and thus processed samples were then scanned by spectrophotometer at A_{254}. Compared to the NT siRNA-treated HeLa cells, $eIF3e^{K.D.}$ showed a decrease in polysomes and enormous increase in the amount of 80S ribosomes as represented by a large monosome peak, which corresponds to translating monosomes and inactive mRNA-unbound 80S couples (Fig. 10.2). The calculated P/M ratios from both cells show that in $eIF3e^{K.D.}$ it dropped by ~ 80 % (P/M = 0.98) as compared to control cells (P/M = 4.88), which indicates severely impaired translation.

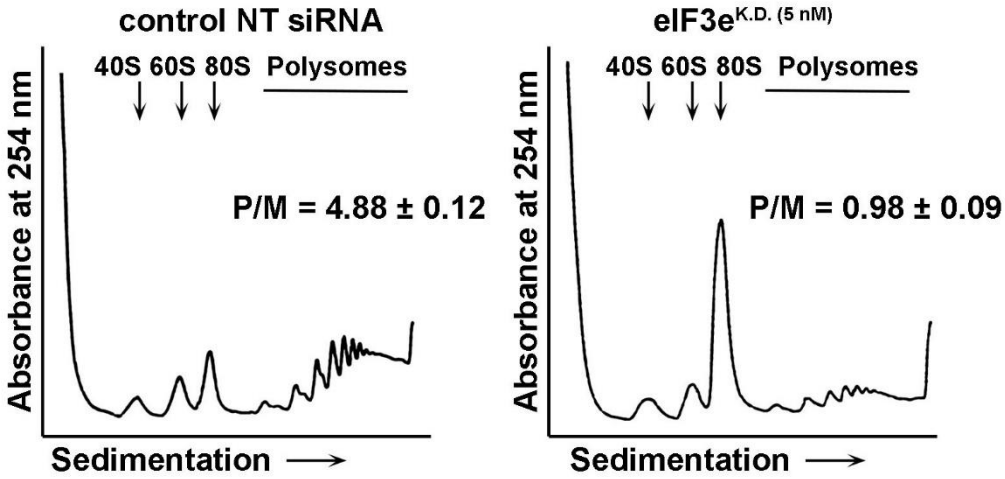

Figure 10.2 Effect of eIF3e knock-down using siRNA at 5nM concentration on translational rates assessed by polysome profile analysis 3 days post-transfection in HeLa cells. To block translation elongation, cells were treated with cycloheximide (100 µg/ml) for 5 min at 37°C prior their harvest. The polysome profile was monitored at A_{254}. Ribosomal subunits (40S and 60S) and 80S ribosomes are indicated with arrows and the polysomes are marked with a bar. Polysome-to-monosome (P/M) ratios represent the mean of three independent experiment and standard deviations are given.

11 Binding of eIF3 to 40S ribosomal subunit in eIF3e knocked-down cells

It was previously shown by our research group that even upon loss of module ii subunits (in $eIF3c^{K.D.}$), the remaining module i and iii subunits are still capable of binding to the 40S subunit, although with reduced affinity, mainly in case of module iii (Wagner et al., 2014). To

find out the consequences of eIF3e$^{K.D.}$, we probed the occupancy of PICs by eIF3 subunits in these siRNA treated cells, applying some modifications of our formerly used method.

Determining which factors are bound to the 40S subunit requires the cells to be treated with a cross-linking reagent to prevent the loss of factors that may occur during high-velocity centrifugation of WCEs in sucrose gradient. Previously, such stabilization of PICs was achieved by incubating the cells with formaldehyde before their lysis, which was shown to work very well at least in yeasts (Valásek et al., 2007). The role of formaldehyde is to basically make a "snap-shot" of any active process in cells, however, we observed that formaldehyde pre-treatment of HeLa cells in the "yeast way" led to a robust decrease of polysomes, which was worrisome. For that reason, we switched to the approach, in which the cross-linking happens during centrifugation of WCEs by adding formaldehyde directly to 7.5 – 30 % sucrose gradient also in a gradient fashion (0 – 0.075 %). We also decreased the speed of centrifugation from the previous 41,000 rpm to the present 22,500 rpm and increased the centrifugation time from 5 hours to 17 hours to allow better separation of 40S ribosomal subunits from lighter factors and heavier ribosomal species. After centrifugation, collected fractions with the last 3 – 4 fractions containing 43S-48S PICs were subjected to Western blotting.

Based on the presence of small ribosomal protein Rps14, the last four fractions in the Western blot profile are denoted as ribosomal fractions containing 43S-48S PICs (Fig. 11.1). In control cells, eIF3 subunits bound to the 40S subunit can be seen in fractions 10 – 12 with the highest signal peak in fraction 11. The 9th fraction could be containing mostly free 40S or partial 43S PICs, as the signal of eIF3 subunits is lower in this fraction. Intact 40S-free eIF3 is distributed mainly across fractions 4 and 5, but residual amount is present also in the fraction 6. Further on top of the gradient (fractions 1 – 3) sediment probably free eIF3 subunits.

In eIF3e$^{K.D.}$, 40S-free intact eIF3 which in control cells´ gradient profile runs in fractions 4 – 6 disappeared and the remaining subunits accumulate in the boxed fractions further documenting the disintegration of eIF3 holocomplex into lighter subcomplexes. The majority of what is left of module ii subunits is either associated with 40S subunits or sediments in the top four fractions. The distribution of non-affected subunits of modules i and iii in ribosomal fractions is shifted by one fraction to the left as there is a clear loss of subunits´ signal in the 12th fraction, which likely indicates that the majority of 43S-48S PICs do not contain all eIF3 subunits and therefore are lighter and sediment earlier in the sucrose gradient. This is expected, since our CoIP experiments showed that module i and module iii stay still connected, but their association is without subunits e, d, k and l not stable enough. The question is then whether module iii can bind to the 40S subunit also by itself or whether it binds always only when

associated with module i. What is obvious from the Western blot picture is that the binding affinity of both modules towards the 40S subunit is decreased. We thus wanted to quantify to what extent does the 40S binding affinity of non-affected subunits of both modules changes upon eIF3e down-regulation.

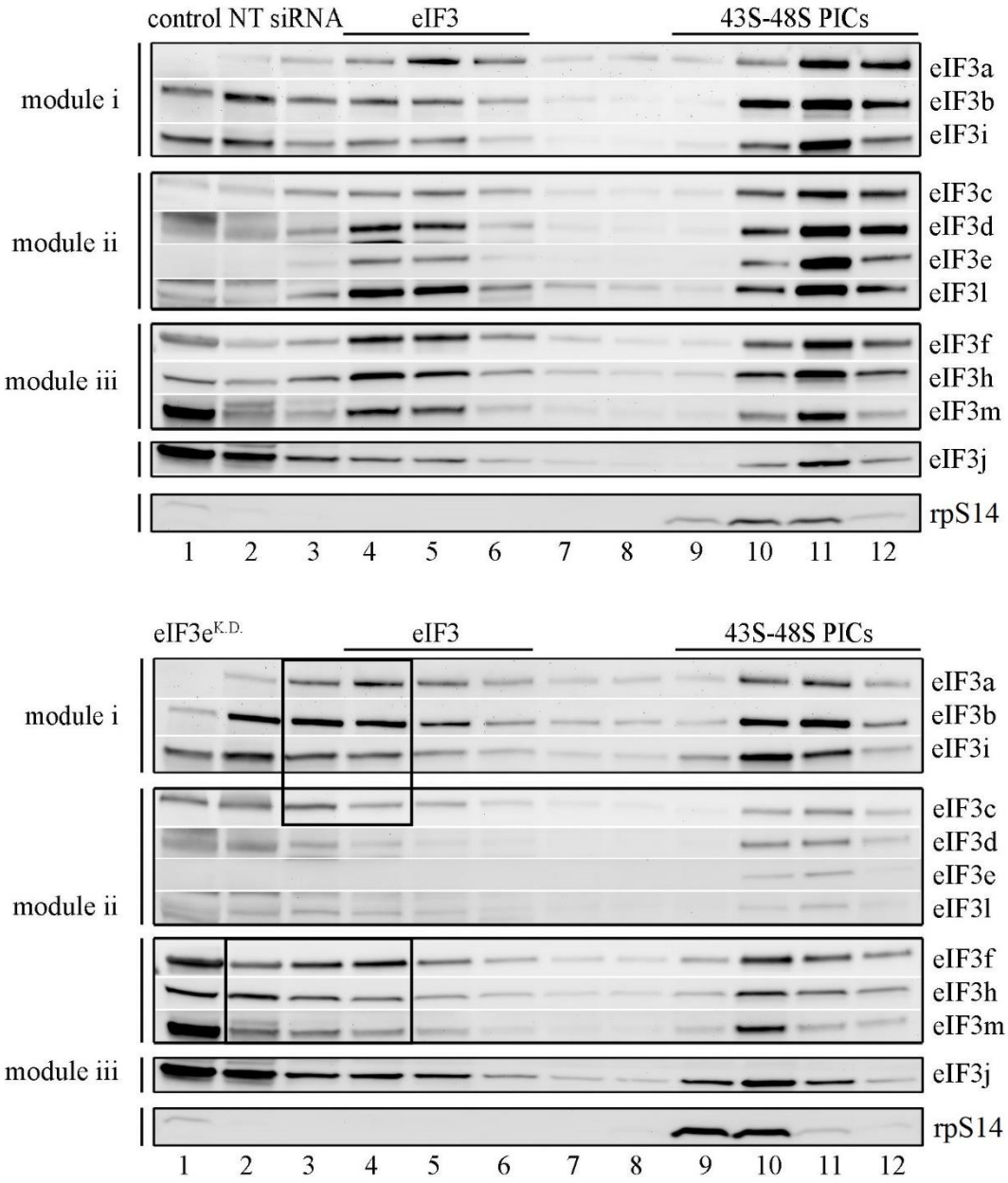

Figure 11.1 Effect of eIF3e downregulation on the ability of other eIF3 subunits to bind to 40S subunit. The experiment was repeated at least three times and the presented picture is from one representative experiment. Fractions containing intact eIF3 and 43S-48S PICs are marked with a line. Boxed fractions are explained in the text.

Standard quantification analysis relies on the normalization of the detected factor´s signal of interest to the signal of rpS14 that represents 40S species. However, in HeLa cells the translation defects resulting from eIF3e$^{K.D.}$ led to the accumulation of the rpS14 signal in 43S-48S ribosomal fractions, which can be already seen in the difference of recorded 40S peaks´ height between NT and eIF3e$^{K.D.}$ (Fig. 11.2 A) as well as in Western blot picture (Fig. 11.1). To find out if it is some kind of a rescue reaction of cells to deficient translation by producing more ribosomes or a result of polysome run-off leading to more free 40S species we measured the protein abundance and found no significant difference in rpS14 signals (Fig. 11.2B). Hence the excess of free 40S subunits (as well as 60S subunits as seen from the recorded profile) in eIF3e$^{K.D.}$ could be only explained by the reduced translation initiation rates as shown by loss of polysomes in polysome profile analysis. Therefore, rpS14 and ribosomal proteins in general are not suitable for the normalization and we had to choose a different quantification approach.

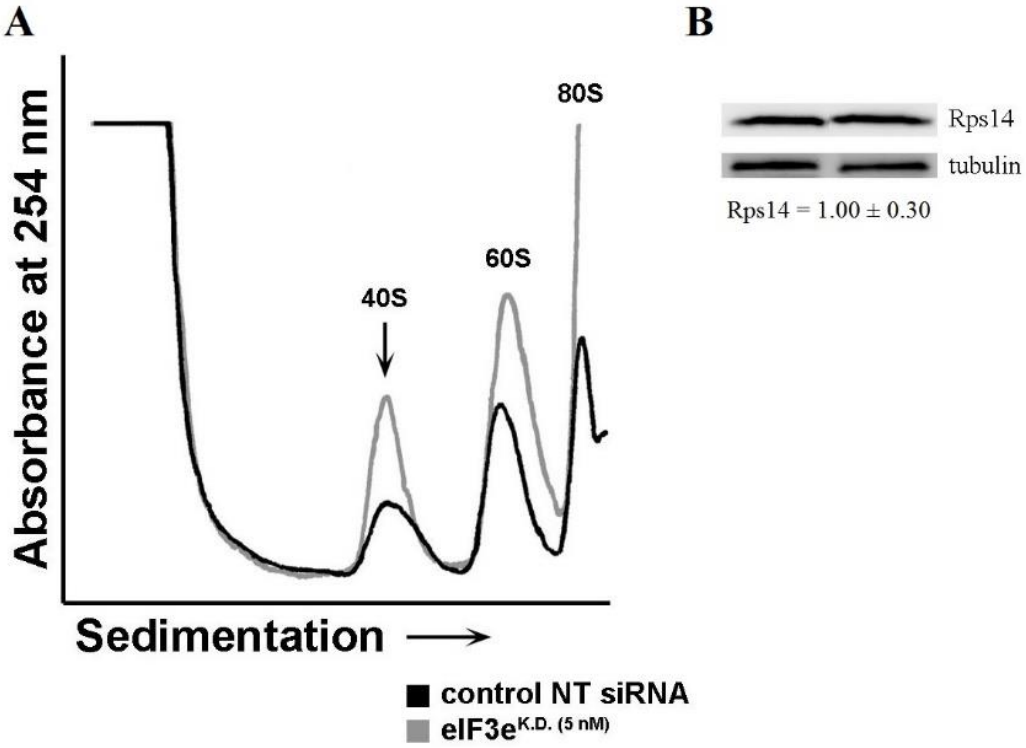

Figure 11.2 Comparison of recorded gradient profile during fractionation of sucrose gradient between control cells and eIF3e$^{K.D.}$. The peak shifts are probably caused by minor variations in sucrose gradients. Depicted curves are representatives from one experiment (A). Protein levels of rpS14 determined by Western blot. Western blotting was repeated at least three times and standard deviation is given (B).

We compared the sucrose density gradient distribution of eIF3 subunits between control and eIF3e$^{K.D.}$ by plotting their distribution curves (Fig. 11.3). The logic behind this was that if the binding affinity of a given subunit decreases upon downregulation of eIF3e, then more of this subunit would sediment in lighter fractions. We focused only on those subunits, whose

protein levels were not affected by this knock-down, so leaving out eIF3e, d, k and l because we expected the residual amounts of these subunits to be either incorporated to the intact eIF3 or bound on the PICs. In general, the NT´s gradient profile exhibits itself in a double-peak fashion, with left peak representing the intact free eIF3 and the right peak representing 40S-bound eIF3. However, there is a clear change in the distribution pattern of all eIF3 subunits but eIF3j in eIF3e$^{K.D.}$. Whereas in NT the highest peak occurs in ribosomal fractions with the distribution curve reaching lower values in top fractions, in eIF3e$^{K.D.}$ there is a clear accumulation of all subunits in the first five fractions at the expense of the 10 – 12 ribosomal peak clearly documenting impaired binding efficiency of eIF3 subunits upon eIF3e downregulation.

Next, we wanted to express this phenomenon in a more quantitative manner. Therefore, the ratio between protein abundance in ribosomal fractions (9 – 12) and the rest of gradient fractions (1 – 8) in eIF3e$^{K.D.}$ was calculated and the resulting amounts in percentages of ribosomal fractions were then expressed as relative to those obtained from control cells (Fig. 11.4). Upon eIF3e knock-down, ~ 40 % of all subunits, except for eIF3j, shifts to the lighter fractions of a sucrose gradient. eIF3b shows somewhat bigger shift (by ~ 60 %), but this can be explained by the troublesome western blot quantification of the 3b signal. In the proximity of the eIF3b-specific band there is another unspecific band, and when quantifying the density of the 3b-specific band, the substracted background is affected by the signal from this unspecific band that artificially decreases the final density value. Unfortunately, we could not answer the question whether module iii can bind to 40S subunit separetely from the rest of eIF3 although our previous work indicates so (Wagner et al., 2014). In case of eIF3e$^{K.D.}$, the binding affinities of both modules i and iii are very similar and further work is needed to resolve the question of module iii separate binding. eIF3j seems to act independently of the rest of eIF3 subunits as its binding to 40S subunit was unaffected. This is consistent with the previous findings, when eIF3j was shown to be able of stable binding to 40S subunit in the absence of other translational factors (Fraser et al., 2004; Wagner et al., 2014).

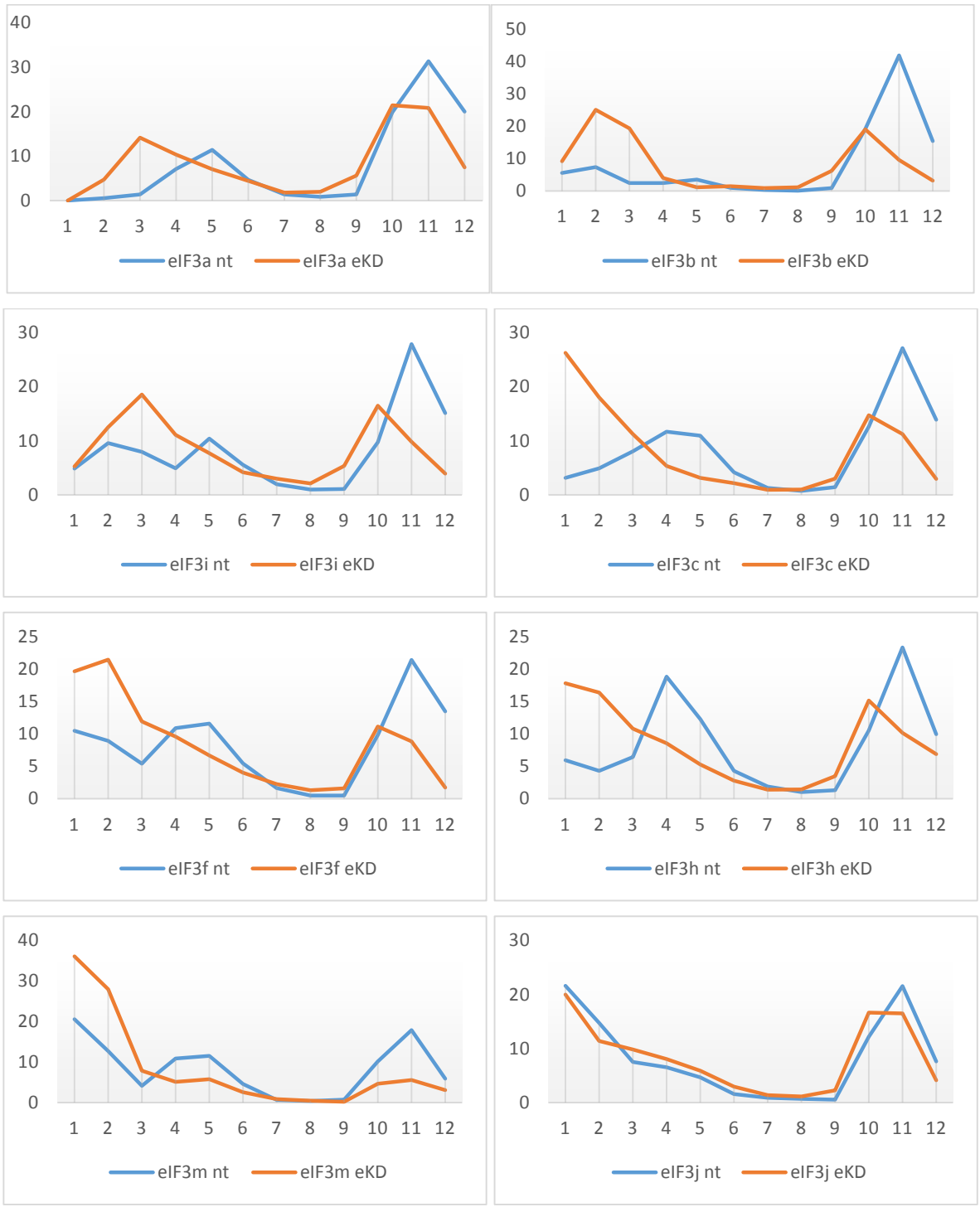

Figure 11.3 Distribution of eIF3 subunits in 7.5 – 30 % continuous sucrose gradient. On the x axis are plotted the numbers of fractions and on y axis is plotted percentual representation of a subunit in respective fraction. The sum of fractions is 100 %.

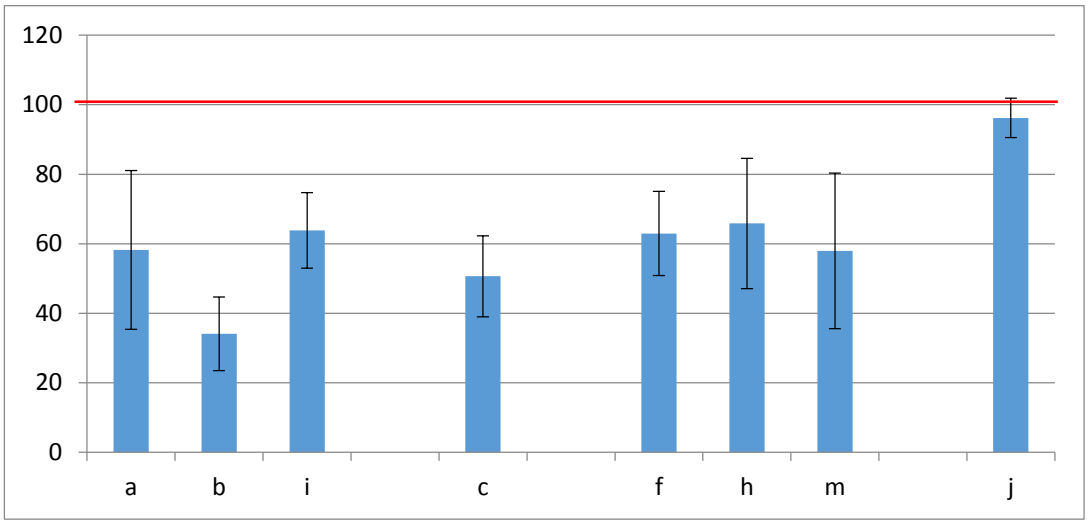

Figure 11.4 Binding efficiency of non-downregulated human eIF3 subunits to 40S ribosome in eIF3e$^{K.D.}$. Obtained values for eIF3e$^{K.D.}$ are expressed as relative to control cells.

Discussion

As eIF3e was shown to occupy the right arm of eIF3 and to be a part of the octameric structural core during the assembly of human eIF3 complex, we wanted to see what effect on the eIF3 integrity would have the depletion of this subunit. To reach this goal, we employed transient transfection of HeLa cells with siRNA pool targeting human eIF3e. Knock-down efficiency was confirmed by severely reduced protein as well as mRNA levels by Western blot and qPCR. Even though this method does not lead to 100 % ablation of the desired gene product, three days after the transfection, when the cells were harvested, we were able to achieve ~ 90 % reduction in eIF3e protein levels. Besides the expected downregulation of targeted eIF3e, we also detected a large drop in protein levels of other three eIF3 module ii subunits, namely eIF3d, k and l. Such an effect, when the depletion of one subunit leads to the loss of other eIF3 subunits, has already been observed in eIF3a, c and m knock-downs (Wagner et al., 2014; Zeng et al., 2013).

In eIF3a$^{K.D.}$, all module ii and iii subunits were affected, whereas in eIF3c$^{K.D.}$ only protein levels of module ii subunits dropped. In case of eIF3m, decreased amounts of eIF3c, f and h were observed, although in this study only 9 out of 13 eIF3 subunits were analysed with eIF3e, g, k and l being omitted. In effort to explain this phenomenon, we first checked the mRNA levels of those subunits, whose protein levels were affected by the eIF3e$^{K.D.}$ to see if the observed reduction could be transcription-related. However, no change in mRNA levels of those subunits was detected suggesting that the drop in the eIF3d, k and l protein levels could be due to either the repression of their mRNA translation or the protein degradation. Protein degradation would appear as a simpler answer, since eIF3e was proposed to make contacts with eIF3d and l, while being connected with eIF3k indirectly via eIF3l (Zhou et al., 2008). Thus, eIF3e depletion could lead to the dissociation of these subunits from eIF3 complex, which would further result in their degradation as their existence outside of the eIF3 complex may lead to their destabilization and targeting for proteolysis. Preliminary experiments to address this question were already done by our postdoc, Susan Wagner. She tried to inhibit the ubiquitin-proteasome proteolytic pathway to find out, if upon knocking-down a specific eIF3 subunit she would prevent the reduction of protein levels of all non-targeted subunits, whose protein levels are otherwise affected by the knock-down. This type of inhibition did not seem to change the outcome of a knock-down. Even though the result was negative, it still does not completely rule out the protein degradation option as the main cause, because proteasome-

mediated proteolysis is not the only proteolytic pathway operating in the cell. Next attempt to resolve this issue would be to examine, if the reduction in protein levels in siRNA-nontargeted eIF3 subunits could be attributed to the regulation on the level of their mRNA translation.

Beside a general stimulating role in translation initiation, human eIF3 was also reported to govern regulation of general gene expression as it was shown to exert either translation activation or repression of specific subset of mRNAs primarily involved in differentiation, proliferation and apoptosis (Lee et al., 2015). Also eIF3h subunit was shown to modulate a specific developmental program during zebrafish embryogenesis by regulating the translation of neural-associated transcripts (Choudhuri et al., 2013). Moreover, in fission yeast, distinct subclasses of eIF3 complexes distinguished by the presence of either eIF3m or eIF3e subunit were shown to regulate specific subsets of mRNAs (Zhou et al., 2005). Hence, perhaps eIF3 is capable of translational regulation also of its own subunits´ mRNAs. To test that, 5´ UTRs of eIF3 mRNAs would need to be cloned in front of a reporter gene, e.g. luciferase and tested for changes in luciferase activity in eIF3 knock-down versus control cells. Then one could search for either a conserved sequence elements or specific secondary structures within these 5´ UTRs. However, the difficulty is that many human eIF3 subunits have annotated more mRNA isoforms in the NCBI database that differ in the length of their 5´UTR. This difference can be probably explained by the cell-type or tissue-specific gene expression, but makes the cloning difficult. The preparation of constructs has already started and is carried out by another postdoc in our research group, Anna Herrmannová, so hopefully this will help us to understand what is behind the loss of other eIF3 subunits upon a specific eIF3 knock-down.

To examine the integrity of human eIF3 upon eIF3e$^{K.D.}$, a WCE extract from eIF3e$^{K.D.}$ cells was subjected to CoIP assay with the antibody against eIF3b subunit. We have previously shown that eIF3c downregulation leads to the separation of module i and module iii, as only module i subunits were retrieved in CoIP with eIF3b as a bait. In eIF3e$^{K.D.}$, protein levels of all module ii subunits except for eIF3c were diminished, which gave us a great advantage for answering the question, if its presence would be enough to hold together module i and iii and thus support its proposed role as a central scaffolding subunit and the main contact point between these two modules (Zhou et al., 2008). Indeed, we were able to pull-down also module iii subunits along with module i, although with lower efficiency than in control cells, but importantly with higher efficiency than we reported for eIF3c$^{K.D.}$ (Wagner et al., 2014). Hence we conclude that even though eIF3c alone is not sufficient for the stable connection of the two modules, it seems that it does represent the main bridging point with one or more module ii subunits further supporting the integrity of the whole complex.

eIF3e was initially identified as a preferred integration site of a mouse mammary tumour virus (Miyazaki et al., 1995). With this finding, however, its association with cancer did not end. Several studies have reported altered expression of eIF3e in various types of cancer tissues, however, its proposed roles in tumour progression remain contradictory. One study has shown elevated protein levels of eIF3e in breast carcinoma cells and that its depletion leads to the reduced proliferation pointing to its oncogenic role (Grzmil et al., 2010). Other studies, however, have shown low expression of this subunit in approximately one third of the examined breast and lung cancer tissue specimen describing it as a potential tumour suppressor (Buttitta et al., 2005; Marchetti et al., 2001). Perhaps, the observed inconsistencies could be explained in a way that in different cell types eIF3e contributes differently to cancerogenesis. In the presented study, silencing of eIF3e by means of its siRNA-mediated knock-down in the HeLa cell line, a cell line derived from ovarian cancer, inhibited the cell proliferation in contrast to HeLa cells treated with NT siRNA. Similar outcome has been also observed in human glioma cells, when downregulation of eIF3e by RNAi technology had a negative impact on the cell growth (Sesen et al., 2014). Surprisingly, reported eIF3e$^{K.D.}$ from three other cell lines derived from glioblastoma (GBM), osteosarcoma (U2OS) or breast cancer (MDA-MB-231) did not exhibit inhibition of global translation as measured by ^{35}S-methionine metabolic labelling (Grzmil et al., 2010; Sesen et al., 2014). In contrast to those findings, our eIF3e$^{K.D.}$ in HeLa cells show massive decrease (almost 5-fold) in translation initiation rates as assessed by polysome profile analysis, which in principle implies nearly complete shutdown of the overall protein synthesis. On the contrary, in lower eukaryotes no apparent defects in translation initiation were observed upon knock-out of eIF3e subunit (a Bandyopadhyay et al., 2000). The aforementioned differences of eIF3e downregulation could be attributed, at least for the human cell lines, to different methodology or that the consequences of eIF3e$^{K.D.}$ could be tissue-specific. It would be interesting to test the effect of eIF3e silencing in HEK293 cells, which are not cancer-derived, although in our previous study they had less pronounced phenotypes when treated with various eIF3 siRNAs than HeLa cells due to less efficient transfectability achieved by siRNA (Wagner et al., 2014). Since in glioma cells it was shown that eIF3e depletion leads to the cell cycle arrest and apoptosis (Sesen et al., 2014), we may also try to test Annexin-V/PI staining followed by flow cytometry to find out if HeLa cells also undergo such physiological changes or not.

Trying to elucidate what impact the eIF3e$^{K.D.}$ had on the assembly of the 43S PIC, we performed 40S binding assay and looked at the representation of eIF3 subunits on the 40S ribosomal subunit. Consistent with our previous findings (Wagner et al., 2014), both modules i

and iii are still capable of binding to the 40S subunit, even though with decreased efficiency. It is in agreement with the recent structures of the 43S PIC, which demonstrated that eIF3 interacts with small ribosomal subunit by two principal contact points via eIF3a and c (Hashem et al., 2013). Surprisingly, the binding of eIF3c to the 40S subunit seems to be the weakest. Also in the CoIP assay it was pulled-down with the lowest efficiency despite its reported interaction with eIF3a and b (Sun et al., 2011; M. Zhou et al., 2008). This is puzzling and so further experiments are needed to elucidate what is behind this.

As the e subunit of human eIF3, together with eIF3c and d, was shown to play an important role in the mRNA recruitment to the ribosome (Villa et al., 2013; Walsh & Mohr, 2014), it would be interesting to examine the efficiency of mRNA binding to the 40S subunit in eIF3e$^{K.D.}$. The major drawback of this knock-down is that the final result is not only a depletion of one subunit and this precludes answering, what is the specific effect of a single eIF3 subunit. Our further effort is to consecutively analyse the knock-down of every human eIF3 subunit, which should hopefully provide us with the complete picture of their cellular roles and their individual contribution to the integrity of eIF3 as well as to the assembly of 43S and 48S PICs.

Conclusions

The presented thesis aimed to explore the importance of the human eIF3e subunit for cell growth by employing the siRNA technology to knock-down the expression of eIF3e in HeLa cells. The observed phenotypes of thus treated cells are summarized here:

i) Efficient knock-down of this subunit revealed the decrease of eIF3e protein by 90 %

ii) eIF3e$^{K.D.}$ led also to the concomitant decrease of protein but not mRNA levels of eIF3d, k and l subunits

iii) The loss of three octameric core subunits (e, k and l) and one non-core subunit (d) in eIF3e$^{K.D.}$ had further impact on the integrity of human eIF3 complex leading to its only partial disintegration into module i and iii thanks to the bridging effect of eIF3c

iv) As this knock-down led to the partial disassembly of one of the main initiation factors, it was not surprising that translation initiation rates were diminished and cell growth ceased

v) Finally, eIF3e$^{K.D.}$ affected the formation of the 43S PIC as expected by reducing the efficiency of the binding of non-affected eIF3 subunits to the 40S ribosome

The obtained results indicate that eIF3e provides considerable structural aid for the integrity of human eIF3 holocomplex that is necessary for promoting the translation initiation.

References

Abdelmohsen, K. (2012). *Modulation of Gene Expression by RNA Binding Proteins: mRNA Stability and Translation*. (K. Abdelmohsen, Ed.). InTech.

Akashi, H. (2003). Translational selection and yeast proteome evolution. *Genetics*, *164*(4), 1291–303. Retrieved from http://www.genetics.org/content/164/4/1291.abstract

Akiyoshi, Y., Clayton, J., Phan, L., Yamamoto, M., Hinnebusch, A. G., Watanabe, Y., & Asano, K. (2001). Fission Yeast Homolog of Murine Int-6 Protein, Encoded by Mouse Mammary Tumor Virus Integration Site, is Associated with the Conserved Core Subunits of Eukaryotic Translation Initiation Factor 3. *Journal of Biological Chemistry*, *276*, 10056–10062.

Asano, K., Clayton, J., Shalev, A., & Hinnebusch, A. G. (2000). A multifactor complex of eukaryotic initiation factors, eIF1, eIF2, eIF3, eIF5, and initiator tRNA(Met) is an important translation initiation intermediate in vivo. *Genes & Development*, *14*(19), 2534–46. Retrieved from http://www.pubmedcentral.nih.gov/articlerender.fcgi?artid=316978&tool=pmcentrez&rendertype=abstract

Asano, K., Phan, L., Anderson, J., & Hinnebusch, A. G. (1998). Complex formation by all five homologues of mammalian translation initiation factor 3 subunits from yeast Saccharomyces cerevisiae. *The Journal of Biological Chemistry*, *273*(29), 18573–85. Retrieved from http://www.ncbi.nlm.nih.gov/pubmed/9660829

Aylett, C. H. S., Boehringer, D., Erzberger, J. P., Schaefer, T., & Ban, N. (2015). Structure of a yeast 40S-eIF1-eIF1A-eIF3-eIF3j initiation complex. *Nature Structural & Molecular Biology*, *22*(3), 269–71.

Bah, A., Vernon, R. M., Siddiqui, Z., Krzeminski, M., Muhandiram, R., Zhao, C., Sonenberg, N., Kay, L. E., & Forman-Kay, J. D. (2014). Folding of an intrinsically disordered protein by phosphorylation as a regulatory switch. *Nature*, *519*(7541), 106–109.

Bandyopadhyay, a, Matsumoto, T., & Maitra, U. (2000). Fission yeast Int6 is not essential for global translation initiation, but deletion of int6(+) causes hypersensitivity to caffeine and affects spore formation. *Molecular Biology of the Cell*, *11*(November), 4005–4018.

Bandyopadhyay, A., Lakshmanan, V., Matsumoto, T., Chang, E. C., & Maitra, U. (2002). Moe1 and spInt6, the fission yeast homologues of mammalian translation initiation factor 3 subunits p66 (eIF3d) and p48 (eIF3e), respectively, are required for stable association of eIF3 subunits. *The Journal of Biological Chemistry*, *277*(3), 2360–7.

Benne, R., & Hershey, J. W. (1976). Purification and characterization of initiation factor IF-E3 from rabbit reticulocytes. *Proceedings of the National Academy of Sciences of the United States of America*, *73*(9), 3005–3009.

Beznosková, P., Cuchalová, L., Wagner, S., Shoemaker, C. J., Gunišová, S., von der Haar, T., & Valášek, L. S. (2013). Translation Initiation Factors eIF3 and HCR1 Control Translation Termination and Stop Codon Read-Through in Yeast Cells. *PLoS Genetics*, *9*(11).

Browning, K. S., Gallie, D. R., Hershey, J. W. B., Hinnebusch, a. G., Maitra, U., Merrick, W. C., & Norbury, C. (2001). Unified nomenclature for the subunits of eukaryotic initiation factor 3. *Trends in Biochemical Sciences*, *26*(5), 284.

Buttitta, F., Martella, C., Barassi, F., Felicioni, L., Salvatore, S., Rosini, S., D'Antuono, T., Chella, A., Mucilli, F., Sacco, R., Mezzetti, A., Cuccurullo, F., Callahan, R., & Marchetti, A. (2005). Int6 expression can predict survival in early-stage non-small cell lung cancer patients. *Clinical Cancer Research : An Official Journal of the American Association for Cancer Research*, *11*(9), 3198–204.

Cuchalová, L., Kouba, T., Herrmannová, A., Dányi, I., Chiu, W.-L., & Valásek, L. (2010). The RNA recognition motif of eukaryotic translation initiation factor 3g (eIF3g) is required for resumption of scanning of posttermination ribosomes for reinitiation on GCN4 and together with eIF3i stimulates linear scanning. *Molecular and Cellular Biology*, *30*(19), 4671–86.

Damoc, E., Fraser, C. S., Zhou, M., Videler, H., Mayeur, G. L., Hershey, J. W. B., Doudna, J. a, Robinson, C. V, & Leary, J. a. (2007). Structural characterization of the human eukaryotic initiation factor 3 protein complex by mass spectrometry. *Molecular & Cellular Proteomics : MCP*, *6*, 1135–1146.

Dennis, M. D., Person, M. D., & Browning, K. S. (2009). Phosphorylation of plant translation initiation factors by CK2 enhances the in vitro interaction of multifactor complex components. *The Journal of Biological Chemistry*, *284*(31), 20615–28.

Dong, Z., Qi, J., Peng, H., Liu, J., & Zhang, J. T. (2013). Spectrin domain of eukaryotic initiation factor 3a is the docking site for formation of the a:b:i:g subcomplex. *Journal of Biological Chemistry*, *288*, 27951–27959.

Elbashir, S. M., Harborth, J., Lendeckel, W., Yalcin, A., Weber, K., & Tuschl, T. (2001). Duplexes of 21-nucleotide RNAs mediate RNA interference in cultured mammalian cells. *Nature*, *411*(6836), 494–8.

Enchev, R. I., Schreiber, A., Beuron, F., & Morris, E. P. (2010). Structural insights into the COP9 signalosome and its common architecture with the 26S proteasome lid and eIF3. *Structure (London, England : 1993)*, *18*(4), 518–27.

Erzberger, J. P., Stengel, F., Pellarin, R., Zhang, S., Schaefer, T., Aylett, C. H. S., Cimermančič, P., Boehringer, D., Sali, A., Aebersold, R., & Ban, N. (2014). Molecular architecture of the 40S·eIF1·eIF3 translation initiation complex. *Cell*, *158*(5), 1123–35.

Fraser, C. S., & Doudna, J. A. (2007). Quantitative studies of ribosome conformational dynamics. *Quarterly Reviews of Biophysics*, *40*(2), 163–89.

Fraser, C. S., Lee, J. Y., Mayeur, G. L., Bushell, M., Doudna, J. A., & Hershey, J. W. B. (2004a). The j-subunit of human translation initiation factor eIF3 is required for the stable binding of eIF3 and its subcomplexes to 40 S ribosomal subunits in vitro. *The Journal of Biological Chemistry*, *279*(10), 8946–56.

Garcia-Garcia, C., Frieda, K. L., Feoktistova, K., Fraser, C. S., & Block, S. M. (2015). Factor-dependent processivity in human eIF4A DEAD-box helicase. *Science*, *348*(6242), 1486–1488.

Georges, A., Dhote, V., Kuhn, L., Hellen, C. U. T., & Tatyana, V. (n.d.). Structure of mammalian eukaryotic Initiation Factor 3 in the context of the 43S preinitiation complex.

Gordiyenko, Y., Schmidt, C., Jennings, M. D., Matak-Vinkovic, D., Pavitt, G. D., & Robinson, C. V. (2014). eIF2B is a decameric guanine nucleotide exchange factor with a γ2ε2 tetrameric core. *Nature Communications*, *5*, 3902.

Grifo, J. A., Tahara, S. M., Morgan, M. A., Shatkin, A. J., & Merrick, W. C. (1983). New initiation factor activity required for globin mRNA translation. *Journal of Biological Chemistry*, *258*(9), 5804–5810. Retrieved from http://www.scopus.com/inward/record.url?eid=2-s2.0-0021099436&partnerID=tZOtx3y1

Grzmil, M., Rzymski, T., Milani, M., Harris, A. L., Capper, R. G., Saunders, N. J., Salhan, A., Ragoussis, J., & Norbury, C. J. (2010). An oncogenic role of eIF3e/INT6 in human breast cancer. *Oncogene*, *29*(28), 4080–9.

Hashem, Y., Des Georges, A., Dhote, V., Langlois, R., Liao, H. Y., Grassucci, R. a., Hellen, C. U. T., Pestova, T. V., & Frank, J. (2013). XStructure of the mammalian ribosomal 43S preinitiation complex bound to the scanning factor DHX29. *Cell*, *153*(5), 1108–1119.

Hershey, J. W. B. (2014). The role of eIF3 and its individual subunits in cancer. *Biochimica et Biophysica Acta (BBA) - Gene Regulatory Mechanisms*.

Hinnebusch, A. G. (2006). eIF3: a versatile scaffold for translation initiation complexes. *Trends in Biochemical Sciences*, *31*(10), 553–562.

Hinnebusch, A. G. (2011). Molecular mechanism of scanning and start codon selection in eukaryotes. *Microbiology and Molecular Biology Reviews : MMBR*, *75*(3), 434–467.

Hinnebusch, A. G., & Lorsch, J. R. (2012). The mechanism of eukaryotic translation initiation: New insights and challenges. *Cold Spring Harbor Perspectives in Biology*, *4*.

Hoareau Alves, K., Bochard, V., Réty, S., & Jalinot, P. (2002). Association of the mammalian proto-oncoprotein Int-6 with the three protein complexes eIF3, COP9 signalosome and 26S proteasome. *FEBS Letters*, *527*(1-3), 15–21. Retrieved from http://www.ncbi.nlm.nih.gov/pubmed/12220626

Hussain, T., Llácer, J. L., Fernández, I. S., Munoz, A., Martin-Marcos, P., Savva, C. G., Lorsch, J. R., Hinnebusch, A. G., & Ramakrishnan, V. (2014). Structural Changes Enable Start Codon Recognition by the Eukaryotic Translation Initiation Complex. *Cell*, 597–607.

Chiu, W.-L., Wagner, S., Herrmannová, A., Burela, L., Zhang, F., Saini, A. K., Valásek, L., & Hinnebusch, A. G. (2010). The C-terminal region of eukaryotic translation initiation factor 3a (eIF3a) promotes mRNA recruitment, scanning, and, together with eIF3j and the eIF3b RNA recognition motif, selection of AUG start codons. *Molecular and Cellular Biology*, *30*(18), 4415–34.

Choudhuri, A., Maitra, U., & Evans, T. (2013). Translation initiation factor eIF3h targets specific transcripts to polysomes during embryogenesis. *Proceedings of the National Academy of Sciences of the United States of America*, *110*(24), 9818–23.

Karásková, M., Gunišová, S., Herrmannová, A., Wagner, S., Munzarová, V., & Valášek, L. S. (2012). Functional characterization of the role of the N-terminal domain of the c/Nip1 subunit of eukaryotic initiation factor 3 (eIF3) in AUG recognition. *The Journal of Biological Chemistry*, *287*(34), 28420–34.

Kolupaeva, V. G., Unbehaun, A., Lomakin, I. B., Hellen, C. U. T., & Pestova, T. V. (2005). Binding of eukaryotic initiation factor 3 to ribosomal 40S subunits and its role in ribosomal dissociation and anti-association. *RNA (New York, N.Y.)*, *11*(4), 470–86.

Korneeva, N. L., Lamphear, B. J., Hennigan, F. L., & Rhoads, R. E. (2000). Mutually cooperative binding of eukaryotic translation initiation factor (eIF) 3 and eIF4A to human eIF4G-1. *The Journal of Biological Chemistry*, *275*(52), 41369–76.

Kozak, M. (1978). How do eucaryotic ribosomes select initiation regions in messenger RNA? *Cell*, *15*(4), 1109–23. Retrieved from http://www.ncbi.nlm.nih.gov/pubmed/215319

Kozak, M. (1987). An analysis of 5'-noncoding sequences from 699 vertebrate messenger RNAs. *Nucleic Acids Research*, *15*(20), 8125–48. Retrieved from http://www.pubmedcentral.nih.gov/articlerender.fcgi?artid=306349&tool=pmcentrez&rendertype=abstract

Lee, A. S. Y., Kranzusch, P. J., & Cate, J. H. D. (2015). eIF3 targets cell-proliferation messenger RNAs for translational activation or repression. *Nature*.

Llácer, J. L., Hussain, T., Marler, L., Aitken, C. E., Thakur, A., Lorsch, J. R., Hinnebusch, A. G., & Ramakrishnan, V. (2015). Conformational Differences between Open and Closed States of the Eukaryotic Translation Initiation Complex. *Molecular Cell*.

Luna, R. E., Arthanari, H., Hiraishi, H., Nanda, J., Martin-Marcos, P., Markus, M. A., Akabayov, B., Milbradt, A. G., Luna, L. E., Seo, H.-C., Hyberts, S. G., Fahmy, A., Reibarkh, M., Miles, D., Hagner, P. R., O'Day, E. M., Yi, T., Marintchev, A., Hinnebusch, A. G., Lorsch, J. R., Asano, K., & Wagner, G. (2012). The C-terminal domain of eukaryotic initiation factor 5 promotes start codon recognition by its dynamic interplay with eIF1 and eIF2β. *Cell Reports*, *1*(6), 689–702.

Maag, D., Algire, M. A., & Lorsch, J. R. (2006). Communication between eukaryotic translation initiation factors 5 and 1A within the ribosomal pre-initiation complex plays a role in start site selection. *Journal of Molecular Biology*, *356*(3), 724–37.

Majumdar, R., Bandyopadhyay, A., & Maitra, U. (2003). Mammalian translation initiation factor eIF1 functions with eIF1A and eIF3 in the formation of a stable 40 S preinitiation complex. *The Journal of Biological Chemistry*, *278*(8), 6580–7.

Marcotrigiano, J., Gingras, A.-C., Sonenberg, N., & Burley, S. K. (1997). Cocrystal Structure of the Messenger RNA 5′ Cap-Binding Protein (eIF4E) Bound to 7-methyl-GDP. *Cell*, *89*(6), 951–961.

Marcotrigiano, J., Lomakin, I. B., Sonenberg, N., Pestova, T. V, Hellen, C. U., & Burley, S. K. (2001). A conserved HEAT domain within eIF4G directs assembly of the translation initiation machinery. *Molecular Cell*, *7*(1), 193–203. Retrieved from http://www.ncbi.nlm.nih.gov/pubmed/11172724

Marchetti, A., Buttitta, F., Pellegrini, S., Bertacca, G., & Callahan, R. (2001). Reduced expression of INT-6/eIF3-p48 in human tumors. *International Journal of Oncology*, *18*(1), 175–9. Retrieved from http://www.ncbi.nlm.nih.gov/pubmed/11115556

Masutani, M., Sonenberg, N., Yokoyama, S., & Imataka, H. (2007). Reconstitution reveals the functional core of mammalian eIF3. *The EMBO Journal*, *26*(14), 3373–3383.

Miyamoto, S., Patel, P., & Hershey, J. W. B. (2005). Changes in ribosomal binding activity of eIF3 correlate with increased translation rates during activation of T lymphocytes. *The Journal of Biological Chemistry*, *280*(31), 28251–64.

Miyazaki, S., Kozak, C. A., Marchetti, A., Buttitta, F., Gallahan, D., & Callahan, R. (1995). The chromosomal location of the mouse mammary tumor gene Int6 and related pseudogenes in the mouse genome. *Genomics*, *27*(3), 420–4.

Morris, C., Wittmann, J., Jäck, H.-M., & Jalinot, P. (2007). Human INT6/eIF3e is required for nonsense-mediated mRNA decay. *EMBO Reports*, *8*(6), 596–602.

Nanda, J. S., Saini, A. K., Muñoz, A. M., Hinnebusch, A. G., & Lorsch, J. R. (2013). Coordinated movements of eukaryotic translation initiation factors eIF1, eIF1A, and eIF5 trigger phosphate release from eIF2 in response to start codon recognition by the ribosomal preinitiation complex. *The Journal of Biological Chemistry*, *288*(8), 5316–29.

Nielsen, K. H., Valásek, L., Sykes, C., Jivotovskaya, A., & Hinnebusch, A. G. (2006). Interaction of the RNP1 motif in PRT1 with HCR1 promotes 40S binding of eukaryotic initiation factor 3 in yeast. *Molecular and Cellular Biology*, *26*(8), 2984–98.

Nunes, E. C., Tamara, D., Lima, C., & Marchini, F. K. (2014). The translation initiation complex eIF3 in trypanosomatids and other pathogenic excavates – identification of conserved and divergent features based on orthologue analysis. *BMC Genomics*, *15*, 1175.

Panniers, R., & Henshaw, E. C. (1983). A GDP/GTP exchange factor essential for eukaryotic initiation factor 2 cycling in Ehrlich ascites tumor cells and its regulation by eukaryotic initiation factor 2 phosphorylation. *The Journal of Biological Chemistry*, *258*(13), 7928–34. Retrieved from http://www.ncbi.nlm.nih.gov/pubmed/6553052

Paulin, F. E. ., Campbell, L. E., O'Brien, K., Loughlin, J., & Proud, C. G. (2001). Eukaryotic translation initiation factor 5 (eIF5) acts as a classical GTPase-activator protein. *Current Biology*, *11*(1), 55–59.

Pestova, T. V, Lomakin, I. B., Lee, J. H., Choi, S. K., Dever, T. E., & Hellen, C. U. (2000). The joining of ribosomal subunits in eukaryotes requires eIF5B. *Nature*, *403*(6767), 332–5.

Phan, L., Schoenfeld, L. W., Valásek, L., Nielsen, K. H., & Hinnebusch, A. G. (2001). A subcomplex of three eIF3 subunits binds eIF1 and eIF5 and stimulates ribosome binding of mRNA and tRNA(i)Met. *The EMBO Journal*, *20*(11), 2954–65.

Phan, L., Zhang, X., Asano, K., Anderson, J., Vornlocher, H. P., Greenberg, J. R., Qin, J., & Hinnebusch, a G. (1998). Identification of a translation initiation factor 3 (eIF3) core complex, conserved in yeast and mammals, that interacts with eIF5. *Molecular and Cellular Biology*, *18*(8), 4935–4946.

Pick, E., Hofmann, K., & Glickman, M. H. (2009). PCI Complexes: Beyond the Proteasome, CSN, and eIF3 Troika. *Molecular Cell*, *35*(3), 260–264.

Pisareva, V. P., Pisarev, A. V, Komar, A. A., Hellen, C. U. T., & Pestova, T. V. (2008). Translation initiation on mammalian mRNAs with structured 5'UTRs requires DExH-box protein DHX29. *Cell*, *135*(7), 1237–50.

Pop, C., Rouskin, S., Ingolia, N. T., Han, L., Phizicky, E. M., Weissman, J. S., & Koller, D. (2014). Causal signals between codon bias, mRNA structure, and the efficiency of translation and elongation. *Molecular Systems Biology*, *10*, 770. Retrieved from http://www.pubmedcentral.nih.gov/articlerender.fcgi?artid=4300493&tool=pmcentrez&rendertype=abstract

Querol-Audi, J., Sun, C., Vogan, J. M., Smith, M. D., Gu, Y., Cate, J. H. D., & Nogales, E. (2013). Architecture of human translation initiation factor 3. *Structure*, *21*, 920–928.

Richter, J. D., & Sonenberg, N. (2005). Regulation of cap-dependent translation by eIF4E inhibitory proteins. *Nature*, *433*(7025), 477–80.

Rogers, G. W., Richter, N. J., Lima, W. F., & Merrick, W. C. (2001). Modulation of the helicase activity of eIF4A by eIF4B, eIF4H, and eIF4F. *The Journal of Biological Chemistry*, *276*(33), 30914–22.

Saini, A. K., Nanda, J. S., Lorsch, J. R., & Hinnebusch, A. G. (2010). Regulatory elements in eIF1A control the fidelity of start codon selection by modulating tRNA(i)(Met) binding to the ribosome. *Genes & Development*, *24*(1), 97–110.

Sesen, J., Cammas, A., Scotland, S. J., Elefterion, B., Lemarié, A., Millevoi, S., Mathew, L. K., Seva, C., Toulas, C., Moyal, E. C.-J., & Skuli, N. (2014). Int6/eIF3e is essential for proliferation and survival of human glioblastoma cells. *International Journal of Molecular Sciences*, *15*(2), 2172–90.

Sha, Z., Brill, L. M., Cabrera, R., Kleifeld, O., Scheliga, J. S., Glickman, M. H., Chang, E. C., & Wolf, D. A. (2009). The eIF3 interactome reveals the translasome, a supercomplex linking protein synthesis and degradation machineries. *Molecular Cell*, *36*(1), 141–52.

Shah, P., Ding, Y., Niemczyk, M., Kudla, G., & Plotkin, J. B. (2013). Rate-limiting steps in yeast protein translation. *Cell*, *153*(7), 1589–601.

Siridechadilok, B., Fraser, C. S., Hall, R. J., Doudna, J. a, & Nogales, E. (2005). Structural roles for human translation factor eIF3 in initiation of protein synthesis. *Science (New York, N.Y.)*, *310*(December), 1513–1515.

Smith, M. D., Gu, Y., Querol-Audí, J., Vogan, J. M., Nitido, A., & Cate, J. H. D. (2013). Human-like eukaryotic translation initiation factor 3 from Neurospora crassa. *PLoS ONE*, *8*(11).

Sokabe, M., & Fraser, C. S. (2014). Human eukaryotic initiation factor 2 (eIF2)-GTP-Met-tRNAi ternary complex and eIF3 stabilize the 43 S preinitiation complex. *The Journal of Biological Chemistry*, *289*(46), 31827–36.

Sokabe, M., Fraser, C. S., & Hershey, J. W. B. (2012). The human translation initiation multi-factor complex promotes methionyl-tRNAi binding to the 40S ribosomal subunit. *Nucleic Acids Research*, *40*(2), 905–13.

Sonenberg, N., & Hinnebusch, A. G. (2009). Regulation of translation initiation in eukaryotes: mechanisms and biological targets. *Cell*, *136*(4), 731–45.

Sun, C., Todorovic, a., Querol-Audi, J., Bai, Y., Villa, N., Snyder, M., Ashchyan, J., Lewis, C. S., Hartland, a., Gradia, S., Fraser, C. S., Doudna, J. a., Nogales, E., & Cate, J. H. D. (2011). Functional reconstitution of human eukaryotic translation initiation factor 3 (eIF3). *Proceedings of the National Academy of Sciences*, *108*(51), 20473–20478.

Svitkin, Y. V, Pause, A., Haghighat, A., Pyronnet, S., Witherell, G., Belsham, G. J., & Sonenberg, N. (2001). The requirement for eukaryotic initiation factor 4A (elF4A) in translation is in direct proportion to the degree of mRNA 5' secondary structure. *RNA (New York, N.Y.)*, *7*(3), 382–94. Retrieved from http://www.pubmedcentral.nih.gov/articlerender.fcgi?artid=1370095&tool=pmcentrez&rendertype=abstract

Tarun, S. Z., & Sachs, A. B. (1996). Association of the yeast poly(A) tail binding protein with translation initiation factor eIF-4G. *The EMBO Journal*, *15*(24), 7168–77. Retrieved from http://www.pubmedcentral.nih.gov/articlerender.fcgi?artid=452544&tool=pmcentrez&rendertype=abstract

Unbehaun, A., Borukhov, S. I., Hellen, C. U. T., & Pestova, T. V. (2004). Release of initiation factors from 48S complexes during ribosomal subunit joining and the link between establishment of codon-anticodon base-pairing and hydrolysis of eIF2-bound GTP. *Genes & Development*, *18*(24), 3078–93.

Valásek, L., Szamecz, B., Hinnebusch, A. G., & Nielsen, K. H. (2007). In vivo stabilization of preinitiation complexes by formaldehyde cross-linking. *Methods in Enzymology*, *429*, 163–83.

Villa, N., Do, A., Hershey, J. W. B., & Fraser, C. S. (2013). Human eukaryotic initiation factor 4G (eIF4G) protein binds to eIF3c, -d, and -e to promote mRNA recruitment to the ribosome. *Journal of Biological Chemistry*, *288*, 32932–32940.

Wagner, S., Herrmannová, A., Malík, R., Peclinovská, L., & Valášek, L. S. (2014). Functional and biochemical characterization of human eukaryotic translation initiation factor 3 in living cells. *Molecular and Cellular Biology*, *34*, 3041–52.

Walsh, D., & Mohr, I. (2014). Coupling 40S ribosome recruitment to modification of a cap-binding initiation factor by eIF3 subunit e. *Genes and Development*, *28*, 835–840.

Wells, S. E., Hillner, P. E., Vale, R. D., & Sachs, A. B. (1998). Circularization of mRNA by eukaryotic translation initiation factors. *Molecular Cell*, *2*(1), 135–40. Retrieved from http://www.ncbi.nlm.nih.gov/pubmed/9702200

Yen, H.-C. S., Gordon, C., & Chang, E. C. (2003). Schizosaccharomyces pombe Int6 and Ras homologs regulate cell division and mitotic fidelity via the proteasome. *Cell*, *112*(2), 207–17. Retrieved from http://www.ncbi.nlm.nih.gov/pubmed/12553909

Zeng, L., Wan, Y., Li, D., Wu, J., Shao, M., Chen, J., Hui, L., Ji, H., & Zhu, X. (2013). Them subunit of murine translation initiation factor eIF3 maintains the integrity of the eIF3 complex and is required for embryonic development, homeostasis, and organ size control. *Journal of Biological Chemistry*, *288*, 30087–30093.

Zhou, C., Arslan, F., Wee, S., Krishnan, S., Ivanov, A. R., Oliva, A., Leatherwood, J., & Wolf, D. a. (2005). PCI proteins eIF3e and eIF3m define distinct translation initiation factor 3 complexes. *BMC Biology*, *3*, 14.

Zhou, M., Sandercock, A. M., Fraser, C. S., Ridlova, G., Stephens, E., Schenauer, M. R., Yokoi-Fong, T., Barsky, D., Leary, J. a, Hershey, J. W., Doudna, J. a, & Robinson, C. V. (2008). Mass spectrometry reveals modularity and a complete subunit interaction map of the eukaryotic translation factor eIF3. *Proceedings of the National Academy of Sciences of the United States of America*, *105*(13), 18139–18144.